

# **Automatic Slip Control for Railway Vehicles**

**Master's thesis**  
performed in **Vehicular Systems**

by  
**Daniel Frylmark and Stefan Johnsson**

Reg nr: LiTH-ISY-EX-3366-2003

6th February 2003



# Automatic Slip Control for Railway Vehicles

Master's thesis

performed in **Vehicular Systems,**  
**Dept. of Electrical Engineering**  
at **Linköpings universitet**

by **Daniel Frylmark and Stefan Johnsson**

Reg nr: LiTH-ISY-EX-3366-2003

Supervisor: **Martin Uneram**

Control Dynamics, Bombardier Transportation,  
Propulsion and Control, Västerås, Sweden

**Fredrik Botling**

Control Products, Bombardier Transportation,  
Propulsion and Control, Västerås, Sweden

**Mattias Eriksson**


Control Products, Bombardier Transportation,  
Propulsion and Control, Västerås, Sweden

Examiner: **Professor Lars Nielsen**

Linköpings universitet

Linköping, 6th February 2003



		<b>Avdelning, Institution</b> Division, Department  Vehicular Systems, Dept. of Electrical Engineering 581 83 Linköping		<b>Datum</b> Date  6th February 2003	
<b>Språk</b> Language <input type="checkbox"/> Svenska/Swedish <input checked="" type="checkbox"/> Engelska/English  <input type="checkbox"/> _____		<b>Rapporttyp</b> Report category <input type="checkbox"/> Licentiatavhandling <input checked="" type="checkbox"/> Examensarbete <input type="checkbox"/> C-uppsats <input type="checkbox"/> D-uppsats <input type="checkbox"/> Övrig rapport <input type="checkbox"/> _____		<b>ISBN</b> _____ <b>ISRN</b> LITH-ISK-EX-3366-2003 <b>Serietitel och serienummer</b> <b>ISSN</b> Title of series, numbering _____	
<b>URL för elektronisk version</b> <a href="http://www.vehicular.isy.liu.se">http://www.vehicular.isy.liu.se</a> <a href="http://www.ep.liu.se/exjobb/isy/2003/3366/">http://www.ep.liu.se/exjobb/isy/2003/3366/</a>					
<b>Titel</b> Slirreglering för spårburna fordon  <b>Title</b> Automatic Slip Control for Railway Vehicles   <b>Författare</b> Daniel Frylmark and Stefan Johnsson <b>Author</b>					
<b>Sammanfattning</b> Abstract  <p>In the railway industry, slip control has always been essential due to the low friction between the wheels and the rail. In this master's thesis we have gathered several slip control methods and evaluated them. These evaluations were performed in MATLAB-SIMULINK on a slip process model of a railway vehicle. The objective with these evaluations were to show advantages and disadvantages with the different slip control methods.</p> <p>The results clearly show the advantage of using a slip optimizing control method, i.e. a method that finds the optimal slip and thereby maximizes the use of adhesion. We have developed two control strategies that we have found superior in this matter. These methods have a lot in common. For instance they both use an adhesion observer and non-linear gain, which enables fast optimization. The difference lies in how this non-linear gain is formed. One strategy uses an adaptive algorithm to estimate it and the other uses fuzzy logic.</p> <p>A problem to overcome in order to have well functioning slip controllers is the formation of vehicle velocity. This is a consequence of the fact that most slip controllers use the velocity as a control signal.</p>					
<b>Nyckelord</b> Adhesion, control, railway vehicle, slide, slip, slip velocity, RLS, fuzzy <b>Keywords</b> logic					



# Abstract

In the railway industry, slip control has always been essential due to the low friction between the wheels and the rail. In this master's thesis we have gathered several slip control methods and evaluated them. These evaluations were performed in MATLAB-SIMULINK on a slip process model of a railway vehicle. The objective with these evaluations were to show advantages and disadvantages with the different slip control methods.

The results clearly show the advantage of using a slip optimizing control method, i.e. a method that finds the optimal slip and thereby maximizes the use of adhesion. We have developed two control strategies that we have found superior in this matter. These methods have a lot in common. For instance they both use an adhesion observer and non-linear gain, which enables fast optimization. The difference lies in how this non-linear gain is formed. One strategy uses an adaptive algorithm to estimate it and the other uses fuzzy logic.

A problem to overcome in order to have well functioning slip controllers is the formation of vehicle velocity. This is a consequence of the fact that most slip controllers use the velocity as a control signal.

**Keywords:** Adhesion, control, railway vehicle, slide, slip, slip velocity, RLS, fuzzy logic





# Acknowledgements

A lot of people deserves credit for their support of this master's thesis. First we would like to thank our supervisors at Bombardier Transportation; Martin Uneram for always taking time for advisory and report reading, Mattias Eriksson, who helped us getting our hands on hard to get data needed in our process model, and Fredrik Botling, who spent a lot of time with us during our simulations and provided a lot of ideas for improvements. Johann Galic at Bombardier Transportation have given us invaluable feedback and support all along the project. We would also like to thank the rest of the staff at PPC/ETD and PPC/ETC at Bombardier Transportation for making us feel like home. Our opponents, Pelle Frykman and Regina Rosander have provided us with a lot of creative feedback and ideas, especially when it comes to the report disposition. The staff at Vehicular Systems, Linköping University, deserve credit for always making us feel welcome. A special thanks to our examiner Lars Nielsen for valuable support and also to Jonas Bitéus and Gustaf Hendeby for the help in L<sup>A</sup>T<sub>E</sub>X-related questions. Finally, we would like to thank our girlfriends for putting up with us always talking about railway vehicles and to ourselves for a well working co-operation. *Thank you all, and may the adhesive force be with you!*

Linköping, February 2003

*Daniel Frylmark & Stefan Johnsson*



# Contents

<b>Abstract</b>	<b>v</b>
<b>Acknowledgments</b>	<b>vii</b>
<b>I Introduction</b>	<b>1</b>
<b>1 Preface</b>	<b>3</b>
1.1 Thesis Background . . . . .	3
1.2 Objectives . . . . .	3
1.3 Methods . . . . .	3
1.4 Method Criticism . . . . .	4
1.5 Organisation . . . . .	4
1.6 Target Group . . . . .	5
1.7 Limitations . . . . .	5
1.8 Time Plan . . . . .	5
1.8.1 Project Planning . . . . .	5
1.8.2 Research Inventory . . . . .	5
1.8.3 Non-Linear Slip Model . . . . .	6
1.8.4 Modelling Control Systems . . . . .	6
1.8.5 Evaluating Control Strategies . . . . .	6
1.8.6 Report Writing . . . . .	6
1.9 Report Disposition . . . . .	6
<b>II Background and Research Inventory</b>	<b>7</b>
<b>2 Theoretical Background</b>	<b>9</b>
2.1 What Makes a Railway Vehicle Move Forward? . . . . .	9
2.2 Adhesive Force . . . . .	10
2.3 Slip, Slip Velocity and Slip Curves . . . . .	12
2.4 Problem Formulation . . . . .	12

<b>3</b>	<b>Slip Control – Techniques and Strategies</b>	<b>15</b>
3.1	Different Ways to Determine the Velocity . . . . .	15
3.1.1	Speed Difference Method . . . . .	17
3.2	Slip Detection . . . . .	17
3.3	Control Strategies . . . . .	18
3.3.1	Neural Networks . . . . .	18
3.3.2	Diagnostic Algorithms . . . . .	18
3.3.3	Detection through Motor Current Differences . . . . .	19
3.3.4	Model Based Controllers . . . . .	19
3.3.5	Hybrid Slip Control Method . . . . .	20
3.3.6	Steepest Gradient Method . . . . .	20
3.3.7	Fuzzy Logic Based Slip Control . . . . .	21
3.4	PID-Controller and its Limitations . . . . .	21
3.5	Summary of Techniques and Strategies . . . . .	22
<b>4</b>	<b>Modelling</b>	<b>23</b>
4.1	Mechanical Transmission . . . . .	23
4.2	Outer Conditions . . . . .	26
4.3	The Train Modelled . . . . .	29
<b>III</b>	<b>Slip Control Packages</b>	<b>31</b>
<b>5</b>	<b>Discussion of Slip Control Methods</b>	<b>33</b>
5.1	Slip Control Method Evaluation . . . . .	33
5.1.1	Hybrid Slip Control Method . . . . .	33
5.1.2	Model Based Controllers . . . . .	34
5.1.3	Fuzzy Logic Slip Controllers . . . . .	34
5.1.4	Strategies not Further Evaluated . . . . .	34
5.2	Test Cycles . . . . .	35
5.2.1	Rail Condition Test . . . . .	35
5.2.2	Acceleration Test . . . . .	36
<b>6</b>	<b>Hybrid Slip Control Method</b>	<b>37</b>
6.1	Control Structure . . . . .	37
6.1.1	Calculations and Control Structure . . . . .	37
6.1.2	Speed Difference Method . . . . .	38
6.1.3	Pattern Control . . . . .	39
6.1.4	Acceleration Criterion . . . . .	40
6.2	Evaluation of the Hybrid Slip Control Method . . . . .	40
<b>7</b>	<b>Model Based Controllers</b>	<b>41</b>
7.1	Derivation of an Adhesion Observer . . . . .	41
7.2	Detection of the Adhesion Peak . . . . .	42
7.3	Slip Control based on an Adhesion Observer . . . . .	43

7.3.1	Direct Torque Feedback Control . . . . .	43
7.3.2	RLS with the Steepest Gradient Method . . . . .	44
7.4	Evaluation of Model Based Controllers . . . . .	48
7.4.1	Direct Torque Feedback Control . . . . .	48
7.4.2	RLS with the Steepest Gradient Method . . . . .	49
<b>8</b>	<b>Fuzzy Logic Slip Controllers</b>	<b>53</b>
8.1	Realization of a Fuzzy Logic Controller . . . . .	53
8.2	Slip Control Methods using Fuzzy Logic . . . . .	54
8.2.1	Fuzzy Logic Non-Linear PD-Controller . . . . .	56
8.2.2	Ideal Fuzzy Logic Slip Optimizing Controller . . . . .	58
8.2.3	Novel Fuzzy Slip Optimizing Controller . . . . .	60
8.3	Evaluation of the Fuzzy Logic Slip Control Methods . . . . .	61
8.3.1	Fuzzy Logic PD-Controller . . . . .	62
8.3.2	Ideal Fuzzy Logic Slip Optimizing Controller . . . . .	64
8.3.3	Novel Fuzzy Slip Optimizing Controller . . . . .	65
<b>9</b>	<b>Conclusions and Future Improvements</b>	<b>69</b>
	<b>References</b>	<b>71</b>
	<b>Notation</b>	<b>75</b>
<b>A</b>	<b>Rail Condition Test, 40 km/h</b>	<b>79</b>



# List of Figures

1.1	Time Plan . . . . .	5
2.1	Slip Process of Car Tires . . . . .	10
2.2	Slip Between the Wheel and the Rail . . . . .	11
2.3	Variation of Adhesion due to Slip . . . . .	13
2.4	Variation of Adhesion due to Vehicle Velocity . . . . .	14
3.1	Railway Vehicle Drive Shaft . . . . .	16
3.2	Block Diagram of Strategies . . . . .	22
4.1	Principle Model of the Mechanical Transmission . . . . .	24
4.2	Maximum Torque Available . . . . .	25
4.3	Mechanical Transmission in Total . . . . .	26
4.4	Slip Curve Model . . . . .	27
4.5	OTU, the Train Modelled . . . . .	30
5.1	Test Curves used . . . . .	36
6.1	Hybrid Slip Control Method . . . . .	38
6.2	Pattern Control . . . . .	39
7.1	Reduced Mechanical Transmission . . . . .	42
7.2	Torque Command Function . . . . .	45
7.3	Block Diagram, Direct Torque Feedback Method . . . . .	45
7.4	Block Diagram, RLS with the Steepest Gradient Method . . . . .	48
7.5	Slip Curve with a Plateau . . . . .	49
7.6	Rail Condition Test for the RLS Method . . . . .	50
7.7	Acceleration Test for the RLS Method . . . . .	51
8.1	Example of Membership Functions . . . . .	54
8.2	Slip Optimizing Algorithm . . . . .	55
8.3	Block Diagram, a Non-Linear PD-Controller . . . . .	56
8.4	Control Surface, a Non-Linear PD-Controller . . . . .	57
8.5	Control Surface, an Ideal Slip Optimizing Controller . . . . .	59
8.6	Block Diagram, an Ideal Optimizing Fuzzy Controller . . . . .	59

8.7	Control Surface, a Novel Optimizing Fuzzy Controller .	61
8.8	Block Diagram, a Novel Optimizing Fuzzy Controller . .	62
8.9	Non-Linear PD-Controller, Rail Condition Test . . . . .	63
8.10	Non-Linear PD-Controller, Acceleration Test . . . . .	64
8.11	Novel Optimizing Controller, Rail Condition Test . . . .	66
8.12	Novel Optimizing Controller, Acceleration Test . . . . .	67
A.1	RLS Method, Rail Condition Test . . . . .	79
A.2	Non-Linear PD-controller, Rail Condition Test . . . . .	80
A.3	Novel Optimizing Controller, Rail Condition Test . . . .	81



## Part I

# Introduction



# Chapter 1

## Preface

### 1.1 Thesis Background

Slipping and sliding have always been major problems in the railway industry, due to the low friction between rail and wheel. Before the days of modern automatic control systems, the skill of the driver set the limits for a successful result. With the increased speed, power and complexity of the modern railway vehicle, the demand for more advanced control systems arises. During the last two decades the automobile industry has developed similar automatic control systems.

Bombardier Transportation in Västerås, Sweden, has offered a master's thesis with the purpose to gather information and to evaluate the recent research. This master's thesis extends to full-time work for two students during 20 weeks. To us, this master's thesis is the final part of our Master of Science education in Applied Physics and Electrical Engineering at Linköpings universitet.

### 1.2 Objectives

To make an inventory of the research progresses within slip control, concerning both the railway and the automobile industry, and evaluate the methods we have encountered as possible strategies for railway vehicles.

### 1.3 Methods

During the first weeks of the project we made a research inventory. The purpose was not only to get the necessary background knowledge, but also to find approaches of automatic slip control that might be useful

for railway vehicles. Based on the gathered information we constructed a MATLAB-SIMULINK model of the non-linear slip process. This model was controlled in MATLAB-SIMULINK, using a few of the strategies we came in touch with during the research inventory, and also a few strategies of our own. The evaluation of their performance as automatic control systems for railway vehicles was put down in this report. The emphasis of this project was to be put on the control strategies and not on the accuracy of the process modelling.

The report is written in L<sup>A</sup>T<sub>E</sub>X 2<sub>ε</sub>. Simulations and calculations were performed in MATHWORKS MATLAB 6.1 (including SIMULINK 4.1). We also used Microsoft Visio Professional for block diagrams and other figures.

## 1.4 Method Criticism

We could have disposed more time on the non-linear process model, but we are firmly convinced that this would not lead to correspondingly better results. Since the focus of this thesis was to find and evaluate different slip control strategies, and not to create one optimal controller, all the methods have not been evaluated to their full extent. Also, all the evaluated methods have not been fully tuned.

## 1.5 Organisation

We have had guidance from Bombardier Transportation in Västerås, as well as from the division of Vehicular Systems, Department of Electrical Engineering at Linköpings universitet. The following persons have taken part in the project:

Professor Lars Nielsen, examiner, Linköpings universitet,  
*lars@isy.liu.se*

Martin Uneram, instructor, Bombardier Transportation, Västerås,  
*martin.uneram@se.transport.bombardier.com*

Mattias Eriksson, instructor, Bombardier Transportation, Västerås,  
*mattias.k.eriksson@se.transport.bombardier.com*

Fredrik Botling, instructor, Bombardier Transportation, Västerås,  
*fredrik.botling@se.transport.bombardier.com*

Stefan Johnsson, master student, Linköpings universitet,  
*stejo483@student.liu.se*

Daniel Frylmark, master student, Linköpings universitet,  
*danfr435@student.liu.se*

## 1.6 Target Group

This is a technical report which turns to readers with basic knowledge in automatic control theory, though it can also be read by others with interest in the subjects treated. However, basic automatic control theory terminology will not be explained in detail.

## 1.7 Limitations

Because of the limited time, it was not possible to evaluate all the strategies we have encountered. All simulations were performed in MATLAB-SIMULINK, since this is the simulation software used at Bombardier Transportation.

## 1.8 Time Plan

Below follows the preliminary time plan for this master's thesis, written in September 2002. The dark grey fields shows where our focus was to be put during specific weeks, but as shown in the light grey regions, our intention was to work simultaneously with several tasks. There has not been any changes in this time plan along the project.

<i>Task</i>	<i>Week</i>																											
	36	37	38	39	40	41	42	43	44	45	46	47	48	49	50	51	52	1	2	3	4	5	6					
Project planning																												
Research inventory																												
Non-linear slip model																												
Modelling control systems																												
Evaluating control strategies																												
Report writing																												

Figure 1.1: The preliminary time plan for this master's thesis.

### 1.8.1 Project Planning

During the first week the time plan of the project was specified in association with the supervisors at Bombardier Transportation.

### 1.8.2 Research Inventory

We spent three weeks of the first month at Linköpings universitet. The research inventory was made both through library research and discussions with scientists at the Department of Electrical Engineering, ISY. The sources of information were both university research and

industrial development within the railway and the automobile industry. The goal of this phase was to conclude which of the automatic control theories we encountered were suitable for railway vehicle slip control.

### 1.8.3 Non-Linear Slip Model

Based on the research inventory, the behaviour of the non-linear slip process was modelled.

### 1.8.4 Modelling Control Systems

We built automatic control systems to control our non-linear slip model.

### 1.8.5 Evaluating Control Strategies

When the control system models were finished we evaluated their performance as possible strategies for slip control. We also looked at possible enhancements and modifications of these control systems.

### 1.8.6 Report Writing

This report was written all along the project, but the last few weeks were fully dedicated to this task. The main objective was to put all the separate pieces together in order to complete the project. By the time the report was finished, a presentation was given in Västerås and another one at Linköpings universitet.

## 1.9 Report Disposition

This report is divided into three parts, starting with this introduction part. The second part consists of three chapters. The first of these chapters treats the theoretical background of the slip phenomenon and the problems concerning slip control. Thereafter follows a brief presentation of the techniques and strategies for slip control we have encountered during our research inventory. Finally there is a chapter describing the process model we have built to evaluate some of these strategies. The third part starts with a short discussion concerning all of the slip control methods treated in the background part. We have divided some of these strategies into three packages and examined them more in detail. The third part of this report ends with a comparison of these slip control methods and a short discussion of improvements that can be made in the future.

## Part II

# Theoretical Background and Research Inventory





## Chapter 2

# Theoretical Background

### 2.1 What Makes a Railway Vehicle Move Forward?

One of the most fundamental theories in vehicle dynamics is the slip theory: *A driven wheel does not roll, but actually rotates faster than the corresponding longitudinal velocity of the vehicle.* As shown in Figure 2.1 the deformation of a car tire causes the reactive normal force to shift horizontally [19].

The difference between the angular velocity of the wheel and the corresponding longitudinal velocity causes the slip. We use the following definition of slip

$$s = \frac{\omega r - v}{v} \quad (2.1)$$

where  $r$  is the radius of the wheel,  $\omega$  the angular velocity of the wheel and  $v$  the longitudinal velocity of the vehicle. The numerator of Equation (2.1) we define as slip velocity  $v_s$ , i.e.

$$v_s = \omega r - v \quad (2.2)$$

Sometimes a separate definition of the slip is used when the slip velocity is negative. This is often called slide, but we choose to refer to it as negative slip.

In railway vehicles the traction procedure is slightly different. First, there are no rubber tires on the wheels, but metal both in the rail and in the wheels. As explained above, the slip is necessary to transmit the motor torque into vehicle movement.

What makes the wheel of the railway vehicle slip? The explanation given by [16] is that due to the massive weight of the railway vehicle, both the wheels and the rail expands and contracts in different regions

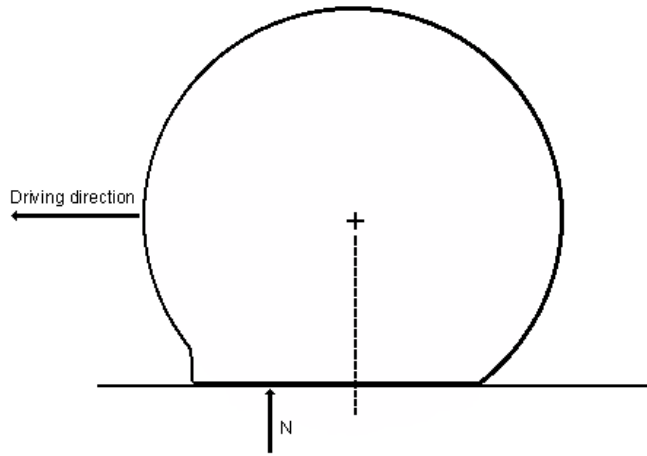


Figure 2.1: How the deformation of a car tire causes the reactive normal force  $N$  to shift horizontally.

when the wheels are driven. This contraction and expansion will make the small slip occur. This phenomenon is shown in Figure 2.2.

## 2.2 Adhesive Force

A general scientific definition of the adhesive force is, *the force of attachment between two contacting objects*. If this definition is translated into a railway definition, it will be the ability of the wheel to exert the maximum tractive force on the rail and still maintain persistence of contact without exceeding the optimal slip [27].

With these definitions it might seem like the adhesive force is equal to the friction force, but this is not the fact. The available adhesion is always lower than the friction between the rail and the track. Parts of the friction are consumed by other friction phenomena [1], such as heat.

Adhesion is *the amount of force available between the rail and the wheel*. Therefore, one can say that the adhesive force comes about as a result of the frictional forces. Further, the friction force is a resistance of motion, and as such an undesirable effect, while adhesion is a coupling

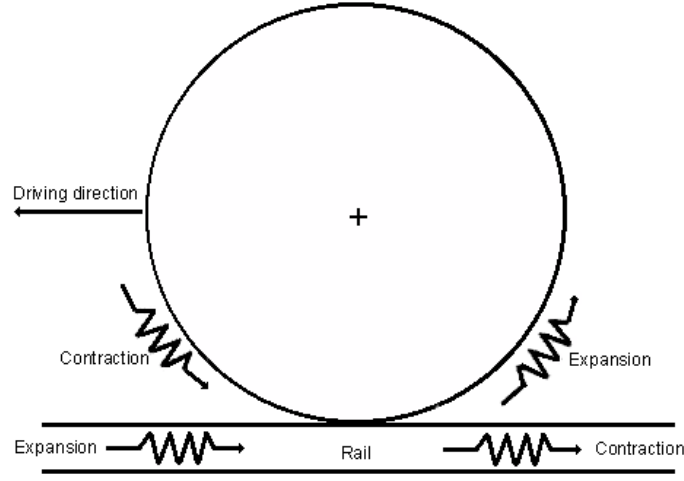


Figure 2.2: How slip occurs between the wheel and the rail.

force and therefore something desirable. The adhesive force is given by

$$F_a = \mu_a N = \mu_a m_a g \quad (2.3)$$

where  $F_a$  is the adhesive force,  $\mu_a$  the adhesion coefficient,  $N$  the normal force,  $m_a$  the adhesive mass of the vehicle and  $g$  the gravitational constant. The adhesive mass is defined by the total mass on all the driven wheels [1]. There may be differences in adhesive mass between wheel axis, depending on the specific load of the trailer et cetera.

The adhesive force  $F_a$  changes in time, though the normal force  $N$  is constant, which implies that the adhesion coefficient  $\mu_a$  changes in time. There are several factors that can affect the value of the adhesion coefficient. Below, a few of them are listed:

- **Contaminants:** Due to the very high stress at the wheel-rail contact point, high adhesion levels could be obtained. This is however not all good. Due to high stress, molecular levels of contaminants can lower the adhesion considerably. Also, larger amounts of contaminants like oil, leaves and moisture (snow, dew and rain) lead to major reductions in adhesion. These factors are random and are therefore hard to model but it is crucial to do so [27].

- **Vehicle velocity:** As the wheels roll along the track, they bounce on surface irregularities. This reduces the normal force between the wheel and the track. Equation (2.3) shows that if the normal force decreases, so will the adhesive force. This phenomenon is difficult to model and would demand a great deal of computational power. In general it can be said that the adhesive force is reduced with increasing vehicle velocity, as shown in Figure 2.4 [27].
- **Slip velocity:** The slip velocity, defined in Equation (2.2), is the most important factor influencing adhesion. The adhesion coefficient becomes higher if the slip velocity is controlled effectively [1]. This means that different reference slip velocities should be used depending on the current rail condition. Much experimental work has been done to derive a general relationship for how slip velocity effects the adhesion coefficient, and thereby the adhesive force [13, 28]. This will be addressed further in Section 2.3.

### 2.3 Slip, Slip Velocity and Slip Curves

As described in Section 2.1, some slip is required in order to transfer the motor torque to vehicle movement. The adhesive force increases when the slip increases, as long as the slip does not become too large. Measurements recently done by [15] confirms that the adhesion coefficient (see Section 2.2) has a peak at a certain slip velocity. This is often presented in figures similar to Figure 2.3. In this figure, the region to the left of the peak is referred to as the stable region, while the right side is called the unstable region.

What is shown in Figure 2.3 is simplified. Measurements have also shown that the adhesion maximum decreases with increasing vehicle velocity [25]. This is illustrated in Figure 2.4.

We have come to the conclusion that slip is used in slip curves in the automobile industry, while the railway industry mostly uses slip velocity. Which one is the better suited for describing the slip phenomenon is disputed. There are also slip models using both. In this case the slip is used in the stable region of the slip curve and the slip velocity in the unstable. This is addressed further in Section 4.2 and described in detail in [25].

### 2.4 Problem Formulation

The goal of all slip control methods is to control the slip in order to prevent wear of the wheels and the rail and to use the present adhesion effectively. Optimizing methods also adds a search of the maximum adhesive force. This is achieved when the slip is controlled towards the

peak of the slip curve. To be able to do this, two major problems must be solved:

- The slip present must be detected.
- The slip must be controlled towards the optimal slip.

Both of these issues are a lot more complex then they might seem at first. This is what will be treated in the rest of this report.

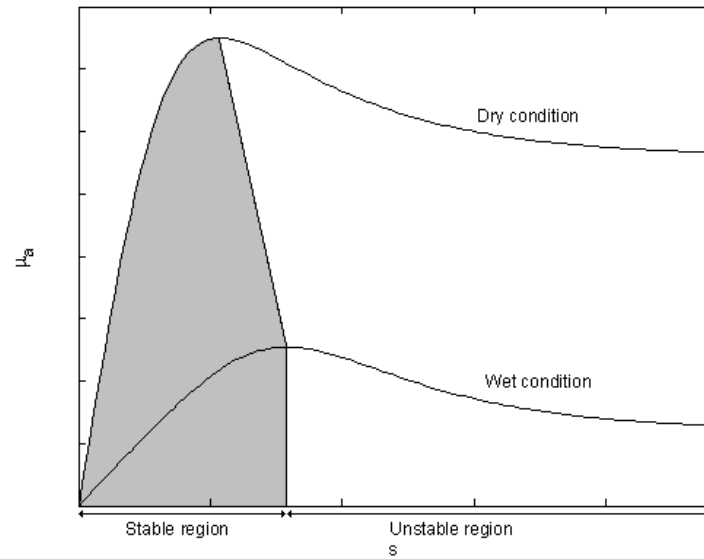


Figure 2.3: How the adhesion between the rail and the wheel varies according to slip.

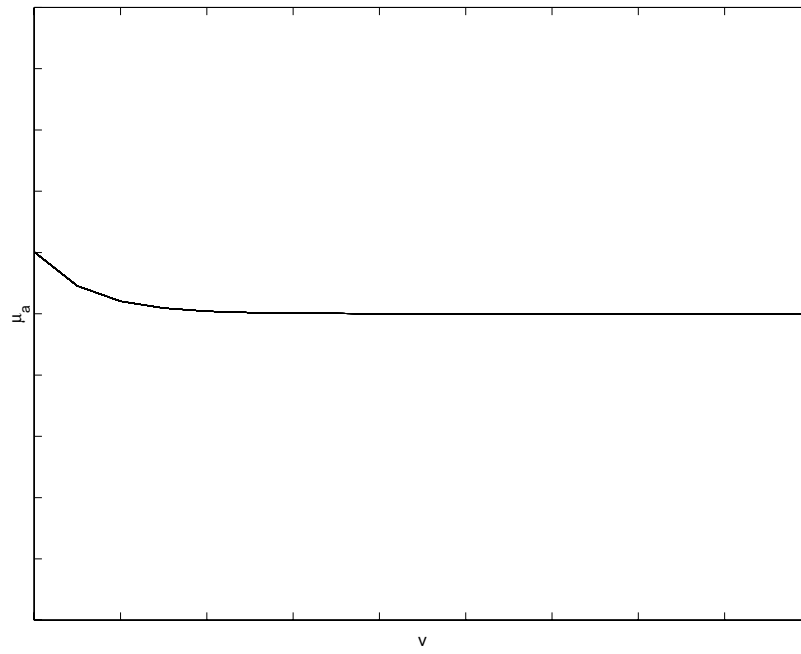


Figure 2.4: How the adhesion coefficient varies with the vehicle velocity.

## Chapter 3

# Slip Control — Techniques and Strategies

There are several problems to overcome to be able to control the slip. Many of the slip control strategies put their focus on detecting the adhesive force or the adhesion coefficient. This can be done in several different ways. We will now present the ideas behind the strategies we have encountered during the research inventory.

### 3.1 Different Ways to Determine the Velocity

If the true velocity of a railway vehicle is known, detecting the slip is fairly easy, and the slip can be controlled by for instance using the steepest gradient method (see Section 3.3.6). The conventional way of calculating a vehicle velocity is to multiply the angular velocity  $\omega$  of a non-driven wheel with the wheel radius  $r$ . In most railway motor cars all wheels are driven, and therefore the use of this method can be fairly complicated, since the speed sensor has to be put on a non-driven shaft, if such a shaft exists. There are however no guarantees this non-driven shaft will never slip, why this method still provides some uncertainty. For instance, mechanical brakes are nowadays considered low-cost and therefore placed on all shafts to increase the braking performance. This may cause uncontrolled negative slip that may lead to brake locking, which will cause massive wheel deformation.

The conventional way of calculating vehicle velocity described above works as follows: A speed sensor is installed at the end of a wheel

shaft or the traction motor shaft. This sensor calculates pulses. The sensors used in many of the Bombardier Transportation railway vehicles calculates between 100 and 120 pulses per revolution. Some believe that the result will be improved significantly by adding the average pulse width into the calculation. This has been done successfully in many years according to [30]. They calculate pulses with a counter frequency of 100 kHz, which gives them a renewal of velocity every 25 ms. They also use this knowledge to calculate the acceleration using velocity differences between the latest calculation made and the one made 100 ms ago. However, others would say that it is not the number of pulses per revolution that is crucial, but whether to trust them or not.

The profile of a railway vehicle wheel is slightly conical (see Figure 3.1). This will help the railway vehicle when turning, since the centripetal force will push the vehicle outwards, which will increase the wheel radius. In time the profile of the wheel will change due to wear and become more weld [1], which of course also will effect the radius. During its entire lifetime, the wheel diameter decreases about 8 %. Manual calibration when a wheel is re-conditioned can be done with an inaccuracy of 1 % [17]. In a modern railway vehicle automatic calibration may be performed on-line.

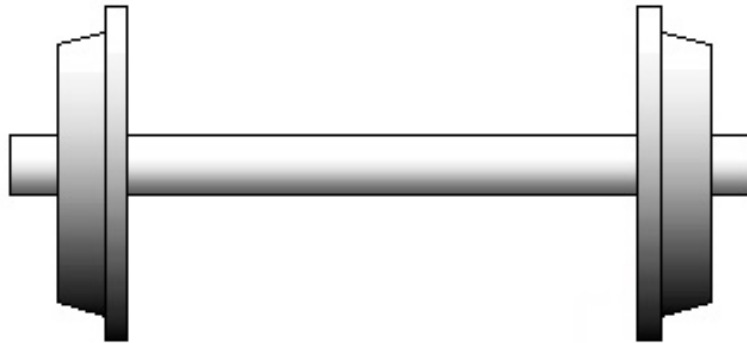


Figure 3.1: A principle railway vehicle drive shaft. Observe the conical profile of the wheels.

In aeroplanes the velocity is determined through a pressure sensor in the front. This method is accurate enough to calculate the aeroplanes approximate velocity, but we doubt it can handle the precision needed for detecting the slip of a railway vehicle. According to [29] the goal is to detect errors of 0.1 km/h in slip velocity, and therefore this is also



what they recommend as a threshold value for slip detection.

GPS might also be a solution to this problem. Hahn et al. [12] have taken this one step further and propose the use of GPS not only for velocity detection but also for slip detection in automobile vehicles. The problems with GPS today are the accuracy and the renewal frequencies. Two other strategies that might be possible for detecting the velocity of a railway vehicle are interference measurements in reflected light and Doppler radars.

### 3.1.1 Speed Difference Method

For reasons described in Section 3.1, it is hard to know the actual velocity of a railway vehicle. Yasuoka et al. [32] proposes the following solution to overcome this problem: Calculate the slip velocity as  $v_s = \omega r - v_{ref}$  (compare with Section 2.1), where  $v_{ref}$  is estimated from the minimum of the angular wheel velocities,  $\omega_{min}$ . The more wheels used to determine the minimum velocity, the higher the accuracy of the reference speed becomes. However, an extra speed sensor on a trailer is probably the best way of increasing the accuracy.

This method has a few disadvantages. If the surface provides low friction for a long time, or if all wheels slip too much simultaneously, this will not be detected [24]. This method is normally used in railway vehicles.

## 3.2 Slip Detection

To be able to control the slip it has to be detected. A few methods to estimate the tire-road friction for an automobile proposed by [10] are:

- Use the differences in velocity of a driven and a non-driven wheel.
- Analyse the vehicles dynamic behaviour.
- Use optical sensors in the front of the vehicle to observe reflections in the surface.
- Let acoustic sensors catch the sound of the tires for analyse.
- Put strain sensors in the tires.

Some of these methods cannot, for obvious reasons, be used for slip detection in railway vehicles. In most railway motor cars all wheels are driven. Therefore the first method mentioned above cannot be used as it is formulated, though a small modification makes it very useful, see Section 3.1.1.

### 3.3 Control Strategies

Below follows a brief description of the different slip control strategies we have come in touch with during our research phase. In Chapter 5 follows a first short evaluation of these methods, there to conclude which of them to continue working with and which of them to leave behind.

#### 3.3.1 Neural Networks

An approach for estimating the parameters that cannot be measured on-line, such as the adhesion coefficient,  $\mu_a$ , is to use neural networks. They can, together with fuzzy control and optimal control theory, be classified as *intelligent transportation systems*. Gadjár et al. [5] have investigated the use of neural networks to estimate  $\mu_a$ . They made simulations using a single wheel unit model of a railway vehicle, claiming that this is sufficient to fully observe the system dynamics. After having simulated this model with  $\mu_a$  varying randomly, they conclude that the most representing signals to be used to estimate  $\mu_a$  is the wheel and vehicle speed differences (see Section 3.1.1) and the angular acceleration of the wheel.

In the simulations, the neural networks were trained by error back propagation. The sample period used was 0.01 seconds and the number of samples in use were 201. They concluded this to be optimal, since an increase of samples would slow down the learning process too much. The net in use have two input signals and one output ( $\mu_a$ ). There are two hidden layers, one with 14 and one with 7 neurons [5].

Gadjár et al. [5] recommend combining neural networks with conventional computation based estimation, for example based upon measurement of the wheel velocity. This partly since the learning process of the neural networks is time consuming. Therefore, this combined method is faster than the use of neural networks alone.

#### 3.3.2 Diagnostic Algorithms

Diagnosis theory can be used to detect the slip. The most simple form is to use so called thresholds, for instance on the slip, that will trigger the control process when exceeded.

Diagnostic algorithms are often combined with observers of various kinds or with consistency relations, which provide information about how the system is expected to behave according to known physical relations [4]. Change detectors can be used to overcome the setback of the slow tracking that linear filters will lead to [9]. These are only a few examples of what might be useful for slip control within the diagnoses research area.

Park et al. [24] uses diagnosis theory in their slip control. They forcibly reduce the motor current when a slip velocity threshold value is exceeded. This method is also known as *the Pattern control method*.

### 3.3.3 Detection through Motor Current Differences

This method is a novel slip control method in the way that it does not use conventional speed sensors. Instead it measures the traction motor current. This can be done since when the rotor speeds of the different traction motors differs from one another, the relevant traction motor current also diverges [31].

According to Watanabe et al. [31] detecting slip through measurements of motor current differences is a well working method. They claim this method to be better at detecting small slips than the conventional method using speed sensors. For example, the differences in wheel diameter due to imbalance or motor characteristics can be compensated for. They believe that it soon will be possible to achieve at least the same adhesive performance without speed sensors as with them.

### 3.3.4 Model Based Controllers

A key to a successful optimizing slip control is to estimate the adhesion coefficient with  $\hat{\mu}_a$  and thereby be able to tell where the peak of the slip curve is [20]. One way of doing this is to use an adhesion observer. The adhesion observer estimates the adhesive torque with  $\hat{T}_a$  through the information given by the motor speed,  $\omega_m$ , and the motor torque,  $T_m$  [22]. Two advantages with adhesion observers are that they have a simple structure and are robust against disturbances and parameter variation. The relationship between the adhesion coefficient and the adhesive torque is given by

$$F_a = \mu_a N \quad (3.1)$$

$$T_a = r F_a \quad (3.2)$$

Here  $N$  is the normal force,  $r$  the radius of the wheel and  $F_a$  the adhesive force. If Equation (3.1) and (3.2) are combined,  $\mu_a$  can be estimated according to

$$\hat{\mu}_a = \frac{1}{rN} \hat{T}_a \quad (3.3)$$

With this information at hand a simple controller can be based on the partial derivative of the adhesion coefficient,  $\frac{\partial \mu_a}{\partial t}$ , together with a PI-controller. We will refer to this method as the direct torque feedback method. Three articles describing this in detail are [20, 21, 22].

Another way of using the adhesion observer is to use the time differential of both the adhesion coefficient,  $\frac{\partial \mu_a}{\partial t}$ , and the slip,  $\frac{\partial s}{\partial t}$ , combined with some adaptive identification algorithm. This enables an on-line estimation of the current slope of the slip curve. In [26] two different algorithms doing this are evaluated.

### 3.3.5 Hybrid Slip Control Method

Park et al. [24] proposes to combine the pattern control method (Section 3.3.2) with the speed difference method (Section 3.1.1). Here, the speed difference method includes a PID-controller, controlling the slip towards a reference slip.

The speed difference method will quickly detect the development of the wheel slip. However, in case of too much slip for a long time, it will fail for reasons described in Section 3.1.1. This is when the pattern control becomes active. If the wheel slip reaches its threshold, the pattern control will forcibly reduce the wheel slip.

This can be even more refined if one also takes acceleration into consideration. The vehicle velocity is only allowed to be increased and decreased at a rate defined by the vehicles maximum acceleration and deceleration. This hybrid method shows remarkably better results than the two methods used separately [24].

### 3.3.6 Steepest Gradient Method

The steepest gradient method is not a complete control method in itself, but more somewhat of a control strategy. It can easily be combined with for instance PID- or fuzzy controllers. The essentials of this method are:

- Estimate the adhesion coefficient with  $\hat{\mu}_a$ . How this can be done is described in Section 3.3.4.
- Estimate the slip  $s$ , defined in Equation (2.1).
- Generate  $\frac{\partial \hat{\mu}_a}{\partial s}$  and control this differential quotient towards zero.

The last step is equivalent with searching for the maximum adhesive force, i.e. the top of the slip curve (see Figure 2.3) [20].

This method can also be applied to the adhesive force  $F_a$  directly. [13] and [15] describe how to estimate the differential quotient according to

$$\frac{\partial F_a}{\partial s} \approx \frac{\partial \hat{F}_a}{\partial t} / \frac{\partial s}{\partial t} \quad (3.4)$$

They also recommend the use of an adhesion observer to estimate the adhesive force  $\hat{F}_a$ . The optimal slip (the reference aimed for) is calculated using

$$v_{s,ref}(t+1) = v_{s,ref}(t) + \alpha \frac{\partial \hat{F}_a}{\partial s} \quad (3.5)$$

where  $\alpha$  is constant. Kawamura et al. [15] uses  $\alpha = 1.0 \times 10^{-5}$ . Equation (3.5) shows that the size of the steps when searching for the optimal slip are non-linear; they are small when close to the optimum and larger when further away.

### 3.3.7 Fuzzy Logic Based Slip Control

Building an effective slip controller is difficult due to the slip being a complex, non-linear and time varying process. Therefore a non-classical methodology, like fuzzy logic based control, is useful. There are several other non-classical methodologies like neural networks and evolutionary algorithms. The disadvantage with these methods is that they rely on numeric or measured data to form system models [2].

One major advantage with fuzzy logic is that it can include experienced human experts linguistic rules, describing how to design the slip control system. These linguistic rules are especially important when the access to measured data is limited. The reason is that they often contain information that is not included in the numerical values. These rules can be translated into IF-THEN rules and in this form be included in the fuzzy logic algorithm.

A fuzzy logic control structure can be tuned simply by changing the weight of some rule. García-Riviera et al. [6] use fuzzy logic to get a fast, non-linear PD-controller, while Palm et al. [23] use it to calculate an optimal slip reference to be controlled towards. More information about fuzzy logic can be found in [3] and [7].

## 3.4 PID-Controller and its Limitations

The proportional-integral-derivative controller (PID) is by far the most used controller in the railway industry today. There are several reasons for this. One is that a PID-controller does not depend on a system model. For more information on how PID-controllers work and are tuned we recommend [7] and [8].

The role of the PID-controller may be to regulate the wheel slip and thereby the use of the adhesive force. A control method can be formulated by examining the adhesion characteristics, see Figure 2.3. This can be done by choosing a reference slip and use this as a control signal. From the characteristics of the slip curve it is easy to observe that different slip, depending on the rail condition, implies different optimums

of the adhesive force. The reason is that the adhesion coefficient differs between dry, wet and icy rail. This is why a PID-controller cannot be used single handed.

As described in Section 2.3, it is important to be on the stable linear side of the slip curve. The optimal position on the slip curve is when the slope is positive and at the same time close to the peak of the adhesive force. But since the adhesion changes in time, so will the optimal position on the slip curve. This is why stability cannot be guaranteed with PID-controllers. An interesting approach would be to combine an adhesion prediction system with a PID-controller, as described in Section 3.3.4 and in Section 3.3.6.

### 3.5 Summary of Techniques and Strategies

All together, most of the methods described in this chapter have quite a lot in common. Few of them use other signals than vehicle velocity and the adhesion as inputs. The differences lie more in how to interpret and process these signals. In Figure 3.2 we have visualized the main features of this chapter.

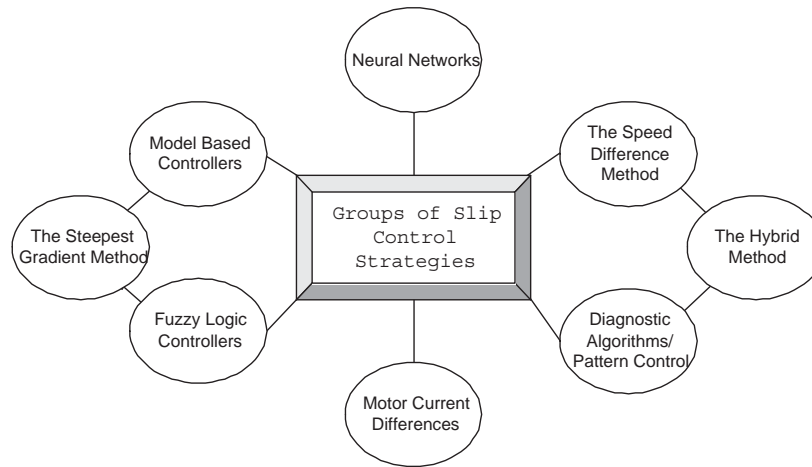


Figure 3.2: The groups of control strategies described in this chapter.

## Chapter 4

# Modelling

To be able to evaluate a few slip control strategies, chosen from the ones described in Chapter 3, a model of the slip phenomenon is necessary. We have developed a dynamic system model with reference torque as input and the velocity of the vehicle as output. This model consists of two fundamental parts. The first is the mechanical transmission, which converts the input torque into the angular velocities of the wheels. The second part consists of the outer conditions, used to produce the present vehicle velocity. This velocity depends on the angular velocities of the wheels, the adhesion present and other losses one might want to take into consideration, such as air resistance, rolling resistance etc.

### 4.1 Mechanical Transmission

The mechanical transmission consists of a traction motor, a gearbox and two wheels. The principle appearance is shown in Figure 4.1. These parts are connected to one another by shafts. We will describe the model part by part, leading towards the total model, shown as a block diagram in Figure 4.3.

#### Traction Motor

To model the torque dynamics of the traction motor and the converter we use a low pass filter

$$T_m = \frac{1}{\tau s + 1} T_{ref} \quad (4.1)$$

where  $T_m$  is the motor torque,  $\tau$  is a time constant and  $T_{ref}$  is the reference torque given by the driver. The maximum reference torque

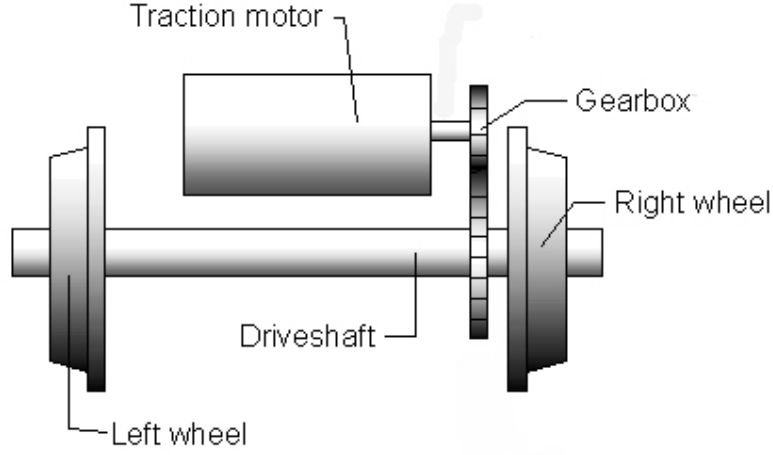


Figure 4.1: The principle appearance of the modelled mechanical transmission, including traction motor, gearbox, shafts and wheels.

accessible is limited according to Figure 4.2. The output torque  $T_t$  of the motor can be described by the following equation

$$J_m \ddot{\theta}_m = T_m - T_t \quad (4.2)$$

$J_m$  is the moment of inertia of the motor,  $\theta_m$  the motor angle,  $T_m$  the input torque and  $T_t$  the output torque.

The output torque of the motor is transmitted to the gearbox by a shaft. This transmission is a function of the angular differences of the shaft on the motor side and on the transmission side and the derivatives of these differences.

$$T_t = K_m(\theta_m - \theta_{t,in}) + \zeta_m(\dot{\theta}_m - \dot{\theta}_{t,in}) \quad (4.3)$$

$K_m$  is the spring constant and  $\zeta_m$  the damping coefficient of the shaft,  $\theta_m$  is the motor angle and  $\theta_{t,in}$  the angle on the gearbox side of the shaft.

#### Gearbox

The gearbox scales the input torque and speed according to a ratio specified as the gear ratio  $i_t$ . In the gearbox there is also a loss due to viscous friction. This is described by the term  $b_t \dot{\theta}_{t,out}$ .  $\theta_{t,in}$  and  $T_t$  are the angle and the torque before the shifting and  $\theta_{t,out}$  and  $T_w$  the



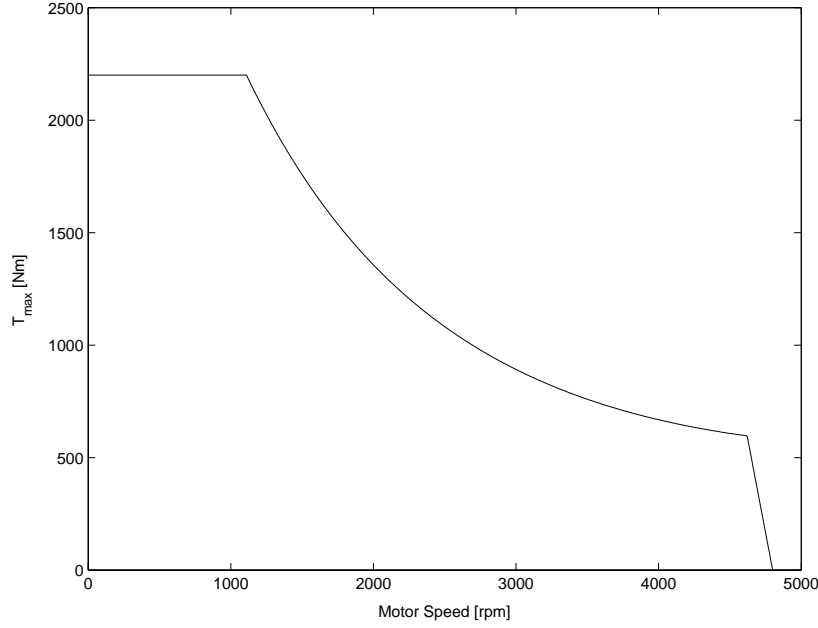


Figure 4.2: The maximum torque available.

angle and the torque after the shifting.  $J_t$  is the moment of inertia of the gearbox.

$$\theta_{t,in} = i_t \theta_{t,out} \quad (4.4)$$

$$J_t \ddot{\theta}_{t,out} = T_t i_t - b_t \dot{\theta}_{t,out} - T_w \quad (4.5)$$

After the gearbox the torque is transmitted to the left and the right wheel via the drive shaft. Since the distance from the gearbox to the left and right wheel are different, so will the spring constants and the damping coefficients of the different sides be. The equation describing the drive shaft torque transmission to one of the wheels is given by

$$T_w = K_t(\theta_{t,out} - \theta_w) + \zeta_t(\dot{\theta}_{t,out} - \dot{\theta}_w) \quad (4.6)$$

$T_w$  is the wheel torque,  $K_t$  the spring constant,  $\zeta_t$  the damping coefficient,  $\theta_{t,out}$  the angle on the gearbox side and  $\theta_w$  the angle on the wheel side of the shaft.

### Wheels

Finally, the wheels will transmit the torque to the rail. This is where the outer conditions appears, since the amount of torque that can be

transmitted depends on the adhesion coefficient as described in Section 2.2.

$$J_w \ddot{\theta}_w = T_w - T_a \quad (4.7)$$

$T_a$  is the adhesive torque, i.e. the adhesive force  $F_a$  multiplied with the radius of the wheel,  $r$ .  $J_w$  is the moment of inertia of the wheel.

#### Mechanical Transmission in Total

Above we have presented all the parts in the mechanical transmission, and how they connect to one another. The result in total is given in the block diagram in Figure 4.3. Notice that we present the wheels separately in this figure. We have implemented the mechanical transmission in MATLAB-SIMULINK following this structure.

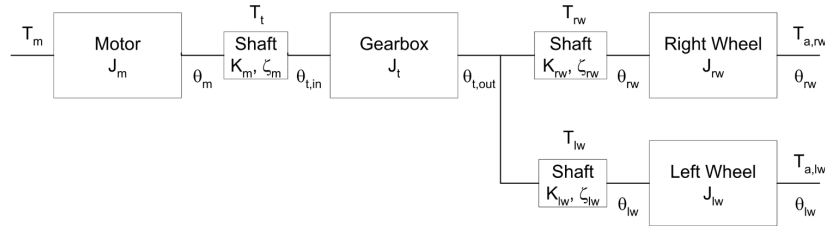


Figure 4.3: The mechanical transmission in total presented as a block diagram.

## 4.2 Outer Conditions

The amount of force that can be transmitted to the rail from the wheels, i.e. the adhesive force  $F_a$ , is determined by what we have chosen to call the outer conditions.

#### Adhesive Force

To model the adhesion coefficient,  $\mu_a$ , we use a slip curve model, containing a few different curves to represent various conditions. Measurements have shown that the adhesion coefficient has a peak at a certain slip velocity [15] and that the maximum value at this peak decreases with increasing vehicle velocity [25]. Whether the slip or the slip velocity is to be used when modelling a slip curve is often discussed. We have chosen to implement a slip curve model with both slip and slip velocity as inputs and the adhesion coefficient as output. The principle behaviour of this model is shown in Figure 4.4.

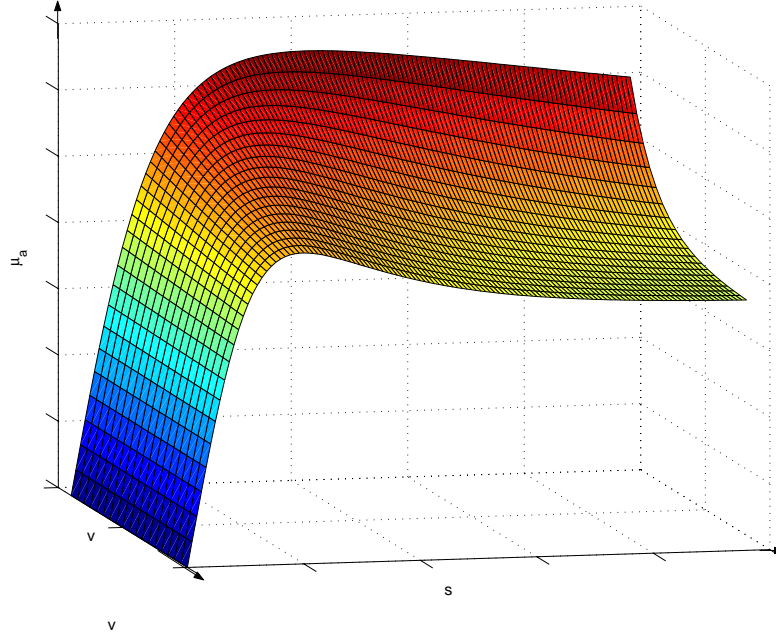


Figure 4.4: The principal behaviour of the slip curve model.

To calculate the slip and the slip velocity for a wheel the angular velocity of the wheel,  $\omega$ , and the vehicle velocity,  $v$ , are needed. The angular velocity is given directly from the mechanical transmission model, described in Section 4.1, since  $\omega = \dot{\theta}_w$ . In our model the vehicle velocity is actually calculated from  $\mu_a$  and fed back into the system. We will return to this later on.

From  $\mu_{a,w}$ , the adhesion coefficient of a specific wheel, the adhesive force of this wheel,  $F_{a,w}$ , is calculated. This is done for both wheels individually according to

$$F_{a,w} = \mu_{a,w} m_{a,w} g \quad (4.8)$$

$m_{a,w}$  is the adhesive mass of this wheel and  $g$  the gravitational constant. Since there are two wheels per drive shaft, the total adhesive force for one drive shaft,  $F_a$ , is the sum of the adhesive forces transmitted from the two wheels.

The adhesive torque,  $T_a = rF_a$  is fed back into the mechanical transmission as described in Equation (4.7). This completes the dynamics of the mechanical transmission part of the model.

### Vehicle Velocity

The velocity of the vehicle is needed for two reasons. Firstly, it is needed in order to be able to calculate  $\mu_a$ . Secondly, it is used in comparison with the wheel velocities when analysing the wheel slip. We calculate the velocity based on Newton's second law of motion:

$$m_{tot}\dot{v} = F_a - F_{loss} \Leftrightarrow v = \int_{t_0}^{t_1} \frac{1}{m_{tot}}(F_a - F_{loss})dt \quad (4.9)$$

The total mass,  $m_{tot}$ , refers to the mass this particular drive shaft has to accelerate, i.e. this is the total mass of the vehicle divided by the number of driven shafts.  $F_{loss}$  is the sum of the outer losses, described below.

### Outer Losses

All of the equations listed in this section have been derived by [1] and [19].  $F_{loss}$  indicates the losses due to roll, air resistance, cornering and the angle of the lateral slope in which the vehicle is currently driving. These losses can be described by

$$F_{loss} = F_{air} + F_r + F_c + m_{tot}g \sin(\varphi) \quad (4.10)$$

The last term,  $m_{tot}g \sin(\varphi)$ , is the loss due to the lateral slope angle  $\varphi$  of the rail.

The loss due to roll,  $F_r$ , depends on the mass of the vehicle,  $m_{tot}$ , and the velocity by which the vehicle is currently driving,  $v$ .

$$F_r = m_{tot}(C_{r1} + C_{r2}v) \quad (4.11)$$

$C_{r1}$  and  $C_{r2}$  are vehicle specific parameters, depending on for instance wheel characteristics.

The cornering loss,  $F_c$ , is the loss due to increased friction between the rail and the wheels when the vehicle is taking a curve. It can be described by the empirical formula

$$F_c = \frac{6.5}{R - 55} m_{tot} \quad (4.12)$$

$R$  is the radius of the curve. This empirical formula is to be seen as an upper limit of the losses. Often the actual cornering loss is limited to 20–70 % of  $F_c$ .

The air resistance is the most complex of the losses

$$F_{air} = \frac{1}{2}C_d A \rho_{air} v^2 + (q + C_0 L_t)v \quad (4.13)$$

$$C_d = C_p + C_l L_t \quad (4.14)$$

$L_t$  is the length of the train,  $\rho_{air}$  the air density and  $A$  the cross section area of the vehicle front.  $C_d$  is the air resistance coefficient. It can be divided into  $C_p$  and  $C_l$ .  $C_p$  depends on the shape of the front section and  $C_l$  on objects along the train, such as the space between wagons.  $q$  is the total ventilation flow.  $C_0$  is the coefficient for aerodynamic phenomenon which cannot be described as functions of  $v^2$ .

In our system model, we have implemented all of the losses, though we neglect them during normal simulation. Both  $F_c$  and  $m_t g \sin(\varphi)$  represent special circumstances; they do not appear when driving straight ahead on flat surface. According to [1], the air resistance does not have any crucial effect for railway vehicles in their normal velocity range, that is up to 160 km/h. Since most slip appear in the low speed region, we chose to neglect the aerodynamics. As the focus in our model is the slip phenomenon, we are convinced that also the roll resistance is insignificant.

### 4.3 The Train Modelled

In order to make this model realistic, there is of course a need for data on the parameters, such as the moment of inertia for each shaft and wheel and, also, the masses in the system. Therefore, a specific railway vehicle had to be selected. We found the Öresund train, OTU (Figure 4.5), suitable for this purpose. OTU operates Malmö and Copenhagen. It is somewhat of a typical electrical multiple unit (EMU). This means that there are traction motors on several driven shafts along the train, instead of having only one locomotive and trailers. OTU comes in units of three cars. These units can be connected in up to five units, which makes it possible to have 15 cars in total. Each unit have eight driven and four non-driven shafts. The driven shafts are placed in the first and the last of the cars in the unit.



Figure 4.5: View of the Öresund train, OTU.

## Part III

### Slip Control Packages — Theory and Evaluation





## Chapter 5

# Discussion of Slip Control Methods

This chapter marks the beginning of the third part of this master's thesis. The second part consisted of the theoretical background and the strategies from the research inventory. In this chapter a discussion will be made about which of these different slip control strategies should be evaluated further.

### 5.1 Slip Control Method Evaluation

If we were able to, we would have implemented and evaluated all of the different slip control methods we have encountered during the research inventory. However, this could not be done, so we had to choose a few of them. One positive thing is that we found that many of the different methods were suitable to combine. We were able to combine the greater parts of these ideas into three different control packages. These three packages will be referred to as the hybrid slip control method, model based controllers and fuzzy logic slip controllers.

#### 5.1.1 Hybrid Slip Control Method

This package, presented in detail in Chapter 6, is similar to the one presented briefly in Section 3.3.5. The so called speed difference method assures fast control of small deviations from the slip wished for. If this deviation becomes too large, the pattern control becomes active, and in case of all-wheel slip, so does the acceleration criterion.

The hybrid slip control method can be refined to any extent by including any of the different strategies described in Chapter 3. However,

we decided to implement it in a basic form, similar to the one described in [24], without any additional optimizing algorithms.

### 5.1.2 Model Based Controllers

In this package, the cornerstone is the observer presented in Section 3.3.4. With this observer as base we have built a few different slip controllers. A common factor in these methods is that they use model equations to detect and control the slip.

There are two main leads in this package for detecting the peak of the slip curve. One is based on  $\frac{\partial \mu_a}{\partial t}$  and the other one use a modified recursive least square algorithm. The first one ends up in a method called the direct torque feedback method, see Section 3.3.4. The latter is combined with the steepest gradient method, see Section 3.3.6. This control package is presented further in Chapter 7.

### 5.1.3 Fuzzy Logic Slip Controllers

The final control package, presented in Chapter 8, consist of three different slip control strategies. What they have in common is the use of a fuzzy logic control surface. The first of them uses fuzzy logic in order to get a fast, non-linear PD-controller, used to control the slip towards the slip reference. The others use fuzzy logic in a slip optimizing algorithm, which calculates an optimal slip reference.

The essence of this control package is the use of fuzzy logic, though a lot of ideas from other strategies in Chapter 3 are used as well. For instance, an adhesion observer and ideas similar to the ones in the steepest gradient method are used in the last of the three control strategies mentioned above.

### 5.1.4 Strategies not Further Evaluated

Due to limitations in both time and literature, we have chosen to exclude further evaluation of two of the strategies from Chapter 3. The first one to be left out was the neural networks strategy, described in Section 3.3.1. The major reasons for leaving this method was the lack of literature, and also our belief that similar results can be achieved with for instance fuzzy logic. The other excluded strategy was the one with slip detection through torque current differences in Section 3.3.3. This strategy was excluded for more or less the same reasons as the neural network strategy. Also, the authors describing this method in [31] do not believe it yet to be possible to achieve the same performance with speed sensorless controllers as with controllers using them. In spite of this, we believe both of these strategies to have great future potentials as slip controllers.

## 5.2 Test Cycles

In order to analyze the strategies we have evaluated further, we need test cycles. The demands on these cycles must be:

- They should be demanding, so that the controllers have to work at their best to handle them.
- They should be repeatable.
- There should be no differences in behaviour when applying the test cycles on the different control strategies.

These demands call for well specified, repeatable tests. Together with our supervisors at Bombardier Transportation, we decided to use the test cycles described in Section 5.2.1 and Section 5.2.2.

### 5.2.1 Rail Condition Test

The essence of this test is to analyse how the controllers handles different types of slip curves, and sudden changes between these curves. The vehicle speed is fixed and so is reference torque, which is set to the maximum reference torque allowed. Two different fixed velocities, 10 and 40 km/h, are used.

#### Test Curves

Firstly, we had to construct slip curves that would not change with the vehicle velocity, as the ones described in Section 4.2 do. This is less realistic, but it will be easier to compare the performance of the different controllers. Two of the curves corresponds to poor and very poor conditions. Their appearances we believe to be quite realistic; the first (curve A) peaks at the slip ratio  $s = 5.4\%$  with  $\mu_{a,max} = 15.0\%$ , while the other (curve B) peaks at  $s = 7.9\%$  with  $\mu_{a,max} = 5.1\%$ . Then, we have a third slip curve (curve C), which is not as realistic as the other two. This curve peaks at  $s = 16.5\%$  with  $\mu_{a,max} = 15.0\%$ . Note that  $\mu_{a,max}$  is the same for this curve as for the first curve, though this peak appears at a higher slip. Its objective is to test the controllers adaptability to unknown rail conditions, under the assumption that the reality is not what it is expected to be. If we would not use such a test curve, many controllers could be tuned to function exemplary for the other two more realistic test curves. Still, we would not know whether or not these controllers could handle unknown conditions. The three test curves are shown in Figure 5.1.

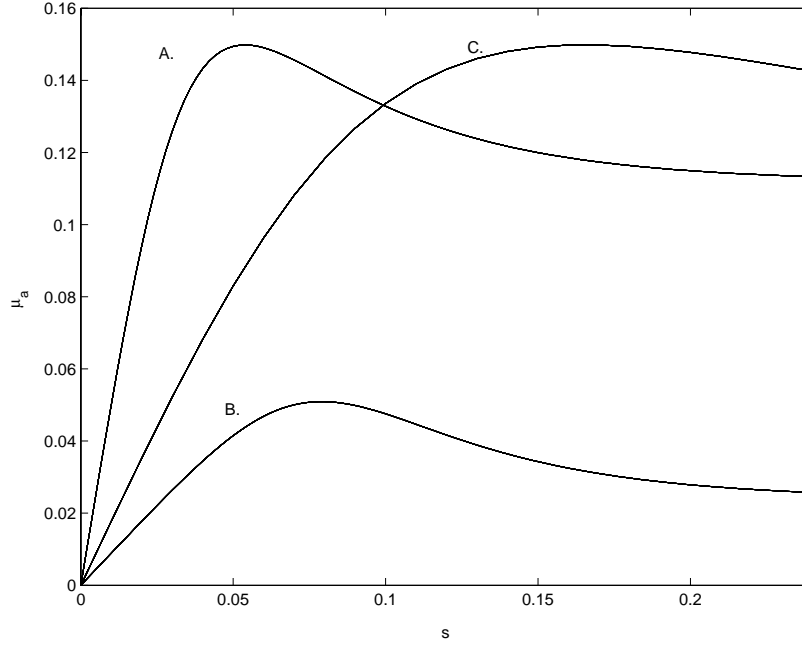


Figure 5.1: The test curves used when evaluating the different control strategies.

#### Test Algorithm

The next step was to formulate the test algorithm. To get the most out of the evaluation, we change between all of the three slip curves in all different orders. Between the changes, the controllers should have enough time to control the slip before another change appears. We have named the three curves A, B and C, and we swap between them every fifth second, starting after ten seconds, in the following order: C-A-B-C-B-A-C. This is done with the reference torque set to maximum and the vehicle velocity fixed at 10 and 40 km/h.

#### 5.2.2 Acceleration Test

The second test is an acceleration test. In this test we use curve B, with  $\mu_{a,max} = 5.1\%$  at  $s = 7.9\%$  (see Figure 5.1), i.e. the worst of our simulated rail conditions. The reference torque is set to its maximum and the initial vehicle velocity is 0 km/h. In this test we compare both the velocity and the performance of the controllers under very bad conditions.

## Chapter 6

# Hybrid Slip Control Method

One of the methods we have evaluated further is the hybrid slip control method. The basic idea is to let direct feedback of the calculated slip handle small slip corrections, while larger ones are handled by the pattern control and the acceleration criterion. The last two are triggered when the calculated slip and acceleration exceeds specific thresholds. Park et al. [24] strongly recommend this approach.

### 6.1 Control Structure

The hybrid slip control method combines two conventional slip control approaches, feedback control and threshold triggered control, into one more powerful control package. The control signals used are the slip velocity and the vehicle acceleration.

#### 6.1.1 Calculations and Control Structure

The slip velocity is calculated by using the angular velocities of the different drive shafts. When accelerating, a reference speed,  $v_{ref}$ , is calculated as the minimum velocity of all the shafts taken into consideration.

$$v_{ref} = \min(v_1, v_2, \dots, v_n) \quad (6.1)$$

When decelerating,  $v_{ref}$  is calculated as

$$v_{ref} = \max(v_1, v_2, \dots, v_n) \quad (6.2)$$

If there is a non-driven shaft present that can be used in this calculation, this will of course improve the result significantly. Park et al. [24] uses

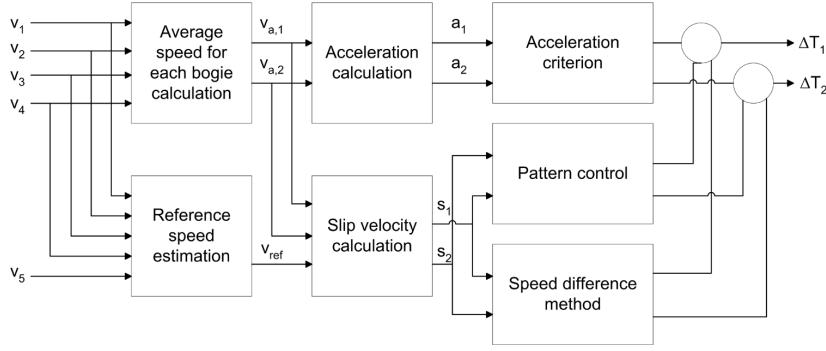


Figure 6.1: Block diagram of the hybrid slip control method. All of the terms used in the diagram are explained in Section 6.1.1.

four driven shafts and one non-driven shaft in their reference speed calculation.

From the velocity of the driven shafts, the average speed for each bogie is calculated. Thereafter the slip velocity is calculated for a bogie as

$$v_{s,i} = v_{a,i} - v_{ref} \quad (6.3)$$

where  $v_{a,i}$  is the average velocity of the specific bogie. This velocity is also used when calculating the acceleration of this bogie. After doing this, all the control signals needed have been calculated.

There are three control blocks in the control structure (Figure 6.1), containing the speed difference method, the pattern control and the acceleration criterion.  $v_1$  and  $v_2$  are the velocities of the shafts in the first bogie and  $v_3$  and  $v_4$  the velocities of the shafts in the second bogie.  $v_5$  represents additional speed information, for instance from a non-driven shaft situated in some other bogie.  $v_{a,1}$  and  $v_{a,2}$  are the average speeds, calculated for each bogie,  $a_1$  and  $a_2$  the accelerations of the bogies.  $\Delta T_1$  and  $\Delta T_2$  are the compensating torques, which shall be subtracted from the reference torque,  $T_{ref}$ .

### 6.1.2 Speed Difference Method

The speed difference method becomes active after a dead zone. It is there to quickly handle small slip corrections, while the pattern control takes care of larger ones. The calculated slip velocity is subtracted from the reference value of the slip velocity, sent through a PI-controller and subtracted from the reference torque,  $T_{ref}$ , to the motor. How to choose this reference value is a problem. It can be set to a small fixed value, expected to guarantee not passing the peak of the present slip curve. On the one hand, setting this value to low will result in a far from

optimal use of the available adhesion. On the other hand, setting it to high will instead lead to wear of both the wheels and the rail, if this reference is on the unstable side of the slip curve (see Figure 2.3). Another solution is to use an algorithm to calculate the optimal slip velocity. How this can be done is described in Chapter 7 and Chapter 8.

### 6.1.3 Pattern Control

The pattern control becomes active if the slip velocity exceeds a specific threshold. If so happens, the reference torque to the motor will be forcibly reduced according to a specific control pattern. The pattern used may have fixed or variable steps. If fixed steps are used, the compensating torque is ramped down for a fixed time period, then constant for short period and finally ramped up again towards zero. This is illustrated in the middle plot in Figure 6.2. In the variable step

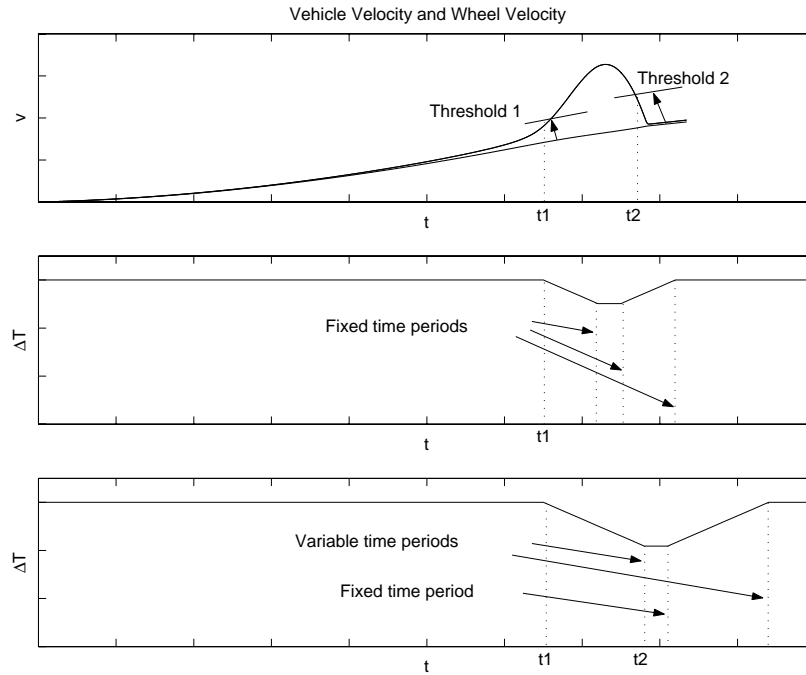


Figure 6.2: When threshold 1 is reached, the reference torque will be forcibly reduced. In the second plot this is done with a fixed step method and in the third plot with a variable step method.

algorithm, the torque will be ramped down until another, lower slip threshold is reached. The behaviour of this algorithm is shown in the third plot in Figure 6.2. When this happens, it will remain low for a

fixed time period and will then be ramped up again towards zero, if the first threshold is not exceeded again. Therefore, also this time period is variable.

#### 6.1.4 Acceleration Criterion

If all the shafts slip uncontrolled simultaneously, neither the speed difference method nor the pattern control will work properly, since they both are in need of a correct vehicle velocity,  $v$ . Therefore, it is important to have an acceleration criterion that reduces the torque when this happens. The acceleration criterion is triggered when an acceleration threshold is exceeded. This threshold is determined by the vehicles maximum acceleration.

## 6.2 Evaluation of the Hybrid Slip Control Method

The hybrid slip control method is well known by Bombardier Transportation. Parts of it is similar to what is used in some of their projects. As we have presented this method, it contains no optimizing parts, i.e. it is controlled towards a fixed slip velocity reference. If the rail conditions are bad, this may cause a lot of trouble, especially if the fixed slip velocity reference chosen is far from what is optimal. Anyhow, we have been told that this type of solution is used for instance in the southern parts of Germany. In these parts, bad rail conditions seldom occur, since there are not a lot of falling leaves near the track and hardly ever ice on the rail.

Since this control method is well known by Bombardier Transportation, we decided together with our supervisors not to put an effort in constructing smart variable step pattern control algorithms (see Section 6.1.3) or tuning this controller. Instead we have focused more on the methods described in Chapter 7 and Chapter 8. Therefore, we will not present any simulation results, since we believe it would be unfair to this method.

The hybrid slip control method is a very interesting control foundation. The different control blocks, i.e. the pattern control etc., can be combined with almost any of the other methods we have looked into. If the slip control in the speed difference method were to be replaced with an optimizing algorithm, this will be a very powerful slip control solution. We also believe that the acceleration criterion can be developed further. For instance, it may be possible to define smart acceleration and deceleration limits based on the reference torque requested by the driver.



## Chapter 7

# Model Based Controllers

This chapter describes and evaluates model based strategies for slip control. There are a few different methods available. What is in common between them is that they all have an observer of the adhesion as base.

### 7.1 Derivation of an Adhesion Observer

The adhesion coefficient,  $\mu_a$ , defined in Section 2.2, can be calculated according to

$$F_a = \mu_a N = \frac{T_a}{r} \iff \mu_a = \frac{F_a}{N} = \frac{1}{Nr} T_a \quad (7.1)$$

where  $N$  is the normal force,  $r$  the radius of the wheel,  $F_a$  the adhesive force and  $T_a$  the adhesive torque. The problem is that the adhesive torque cannot be measured. To solve this, an adhesion observer will be derived.

In Chapter 4 the necessary equations for an adhesion observer were presented. To simplify these equations, the shafts in the mechanical transmission are assumed to be stiff according to Figure 7.1. This assumption reduces the mechanical transmission equations to

$$J_m \ddot{\theta}_m = T_m - T_t \quad (7.2a)$$

$$\theta_m = \theta_{t,in} \quad (7.2b)$$

$$\theta_{t,in} = i_t \theta_{t,out} \quad (7.2c)$$

$$J_t \ddot{\theta}_{t,out} = T_t i_t - b_t \dot{\theta}_{t,out} - T_w \quad (7.2d)$$

$$\theta_{t,out} = \theta_{lw} \quad (7.2e)$$

$$\theta_{t,out} = \theta_{rw} \quad (7.2f)$$

$$J_{lw} \ddot{\theta}_{lw} + J_{rw} \ddot{\theta}_{rw} = T_w - T_a \quad (7.2g)$$

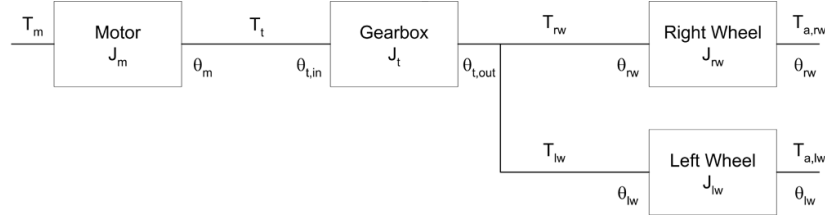


Figure 7.1: The reduced block diagram of the mechanical transmission. Here the shafts are assumed to be stiff and thereby the shaft dynamics can be overlooked. Compare with Figure 4.3

By combining the equations in Equation (7.2), and thereby eliminate the intermediate variables, the following equation is deduced

$$J_{tot}\ddot{\theta}_m = i_t^2 T_m - b_t \dot{\theta}_m - i_t T_a \quad (7.3)$$

The total moment of inertia,  $J_{tot}$ , is deduced to

$$J_{tot} = J_m i_t^2 + J_t + J_{lw} + J_{rw} \quad (7.4)$$

The adhesive torque can be extracted from the Equation (7.3) which results in the following equation

$$T_a = i_t T_m - \frac{b_t}{i_t} \dot{\theta}_m - \frac{J_{tot}}{i_t} \ddot{\theta}_m \quad (7.5)$$

By adding a lowpass filter, the minimal order observer can be deduced to

$$\hat{T}_a = \frac{\omega_c}{s + \omega_c} (T_m - b_t \dot{\theta}_m - J_{tot} \ddot{\theta}_m) \quad (7.6)$$

Here  $\omega_c$  is both the pole and the cut-off frequency of the observer and at the same time the only tunable parameter. Through simulations we have found that  $\omega_c = 100$  results in a satisfactory observer. In other words, a suitable combination of sensitivity and speed of the observer. This also agrees with what we have found in the literature, for example in [14] and [15]. If the Equations (7.1) and (7.6) are combined, the adhesion coefficient can be calculated according to

$$\hat{\mu}_a = \frac{1}{N_r} \hat{T}_a \quad (7.7)$$

## 7.2 Detection of the Adhesion Peak

The adhesion coefficient is a function of the slip velocity. This relationship is often shown in slip curves, see Section 2.3. The slope of

these slip curves are equal to  $\frac{\partial \mu_a}{\partial v_s}$ . Both  $\mu_a$  and  $v_s$  are time dependent variables, hence the following result can be achieved by the use of the chain rule

$$\frac{\partial \mu_a}{\partial v_s} = \frac{\partial \mu_a}{\partial t} \bigg/ \frac{\partial v_s}{\partial t}, \quad \text{if} \quad \frac{\partial v_s}{\partial t} \neq 0 \quad (7.8)$$

The problem is that  $\frac{\partial \mu_a}{\partial t}$ , due to  $\mu_a$ , cannot be measured. This is solved by differentiating the adhesive torque of the adhesion observer, Equation (7.6). The adhesion coefficient is then calculated from Equation (7.7). Therefore, the slope of the slip curve can be calculated through

$$\frac{\partial \hat{\mu}_a}{\partial v_s} \approx \frac{\partial \hat{\mu}_a}{\partial t} \bigg/ \frac{\partial v_s}{\partial t} \quad \text{if} \quad \frac{\partial v_s}{\partial t} \neq 0 \quad (7.9)$$

At the peak of the slip curve the following is fulfilled

$$\frac{\partial \mu_a}{\partial v_s} = 0 \iff \frac{\partial \hat{\mu}_a}{\partial t} \bigg/ \frac{\partial v_s}{\partial t} = 0 \quad \text{if} \quad \frac{\partial v_s}{\partial t} \neq 0 \quad (7.10)$$

This is developed further in the articles [20, 21, 22] in the following way: If

$$\frac{\partial \mu_a}{\partial t} \bigg/ \frac{\partial v_s}{\partial t} = 0 \quad (7.11)$$

then  $\frac{\partial \mu_a}{\partial t}$  must equal zero according to Equation (7.10). Hence the peak of the slip curve can be detected simply by examining  $\frac{\partial \mu_a}{\partial t}$ . According to [20], the timing point of  $\frac{d\mu_a}{dt} = 0$  and  $\frac{dv_s}{dt} = 0$  is almost identical and therefore it is enough to examine when  $\frac{d\mu_a}{dt} = 0$  to detect the peak of the slip curve. This approach is interesting, because if it is successful the peak of the slip curve can be detected without calculating the actual slip velocity. This means there is no need for measuring the vehicle velocity. This is a huge advantage, since the velocity of the vehicle is difficult and often troublesome to measure. In Section 7.3.1 this method will be examined further and developed into a complete control method.

### 7.3 Slip Control based on an Adhesion Observer

There are several ways to use the adhesion observer in Equation (7.6) for slip control. Below two of the ones we found interesting are presented.

#### 7.3.1 Direct Torque Feedback Control

This method, like any other slip optimizing control method, has the control goal of maximizing the use of the adhesion coefficient. But

unlike the other methods, this approach uses the fact that at the peak of the slip curve  $\frac{\partial \mu_a}{\partial t} = 0$ , according to the discussion in Section 7.2. The interesting thing with this method is that it detects the peak of the slip curve without using any slip calculations. This strategy is therefore independent of the vehicle velocity.

One way of using this was realised by [21] with the use of a PI-controller.

$$T_{PI} = \frac{K_I + K_P s}{s} \cdot s \mu_a = K_I \mu_a + K_P s \mu_a \quad (7.12)$$

$K_I$  is the gain of the integrating part of the PI-controller controller and  $K_P$  the gain of the proportional part.  $T_{PI}$  is the reference torque that is fed back. If Equation (7.1) is applied to Equation (7.12) the following result is obtained

$$T_{PI} = \frac{K_I}{N r_w} T_a + \frac{K_P}{N r_w} \dot{T}_a \quad (7.13)$$

This PI-controller, Equation (7.13), is useful in the stable region of the slip curve. However, in the unstable region it is difficult for this PI-controller to keep the desired locus of operation point slightly below the peak on the stable side. To be able to handle this and large variations in the adhesion coefficient, i.e. different rail conditions, [22] proposes a torque command function  $C(t)$ . This function rapidly lowers the motor torque and then smoothly recovers it according to Figure 7.2. The torque command function is added to  $T_{PI}$ , Equation (7.13). The complete control loop is realized according to the block diagram in Figure 7.3.

### 7.3.2 RLS with the Steepest Gradient Method

#### Rail Condition Estimator

This method uses the fact that the slope of the slip curve,  $k$ , is given by  $\frac{\partial \mu_a}{\partial s}$  and therefore, as been described in Section 7.2, can be expressed by

$$k = \frac{\partial \mu_a}{\partial s} = \frac{\partial \mu_a}{\partial t} \bigg/ \frac{\partial s}{\partial t} \quad (7.14)$$

The problem is that both  $\frac{\partial \mu_a}{\partial t}$  and  $\frac{\partial s}{\partial t}$  are signals with noise. Another even bigger problem is when the peak is closing in,  $\frac{\partial s}{\partial t}$  turns to zero. When this occurs it cannot divide  $\frac{\partial \mu_a}{\partial t}$ . One solution to this problem is to use an adaptive identification algorithm. Equation (7.14) is suitable for the use of various adaptive identification algorithms.

A way of implementing an adaptive identification algorithm is presented in [26]. For a further presentation of identification algorithms see [11] and for an in depth presentation see [18]. One algorithm that

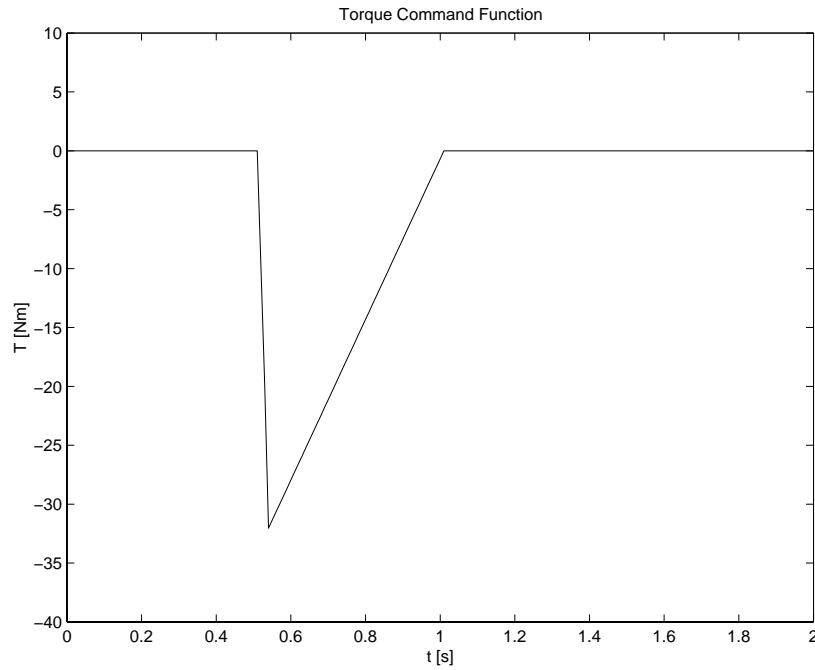


Figure 7.2: Torque command function,  $C(t)$ . This function rapidly lowers the torque and then smoothly recovers it.

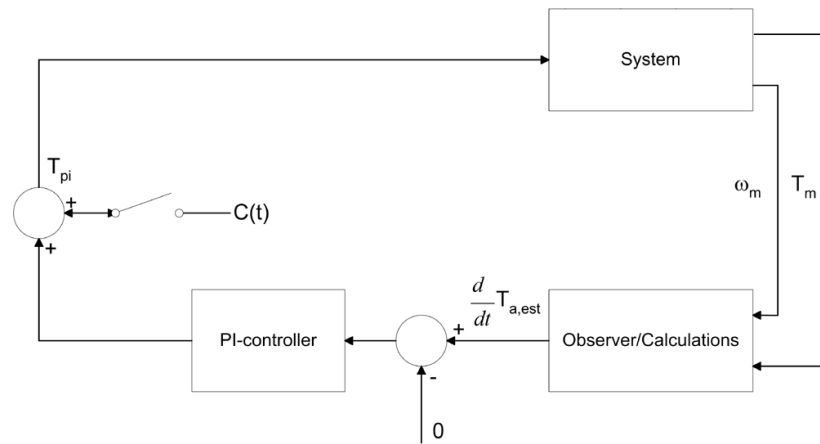


Figure 7.3: Block diagram of the direct torque feedback method.

we have implemented is the recursive least square (RLS) with a dynamic forgetting factor. The algorithm is formulated as follows

$$y(t) = \varphi(t)^T \theta(t) \quad (7.15a)$$

$$\hat{\theta}(t) = \hat{\theta}(t-1) + Q(t)[y(t) - \varphi(t)^T \hat{\theta}(t-1)] \quad (7.15b)$$

$$Q(t) = P(t)\varphi(t) \quad (7.15c)$$

$$P(t) = \frac{1}{\lambda} \left[ P(t-1) - \frac{P(t-1)\varphi(t)\varphi^T(t)P(t-1)}{\lambda + \varphi^T(t)P(t-1)\varphi(t)} \right] \quad (7.15d)$$

$$\lambda = \frac{1}{1 + \gamma\varphi(t)^2} \quad (7.15e)$$

Equation 7.15 is a combination of the algorithms presented in [11] and [26]. A rail condition estimator can be designed by giving the estimation parameters according to

$$\varphi(t) = \frac{\partial s}{\partial t} \quad (7.16a)$$

$$y(t) = \frac{\partial \mu_a}{\partial t} \quad (7.16b)$$

$$\hat{\theta}(t) = k \quad (7.16c)$$

By inserting Equation (7.16) into the RLS algorithm and using the fact that the signals are scalars and not vectors, the RLS algorithm can be reduced to

$$\frac{\partial \mu_a}{\partial t} = \frac{\partial s}{\partial t} k \quad (7.17a)$$

$$\hat{k}(t) = \hat{k}(t-1) + Q(t) \left[ \frac{\partial \mu_a}{\partial t} - \frac{\partial s}{\partial t} \hat{k}(t-1) \right] \quad (7.17b)$$

$$Q(t) = P(t) \frac{\partial s}{\partial t} \quad (7.17c)$$

$$P(t) = \frac{1}{\lambda} \left[ P(t-1) - \frac{P^2(t-1) \left( \frac{\partial s}{\partial t} \right)^2}{\lambda + P(t-1) \left( \frac{\partial s}{\partial t} \right)^2} \right] \quad (7.17d)$$

$$\lambda = \frac{1}{1 + \gamma \left( \frac{\partial s}{\partial t} \right)^2} \quad (7.17e)$$

The special thing with this version of the RLS algorithm is the dynamic forgetting factor  $\lambda$  in Equation (7.15e).  $\lambda$  decides how many of the previous values that will be taken into account when the next value is estimated. If  $\lambda$  is near 1 the RLS will remember all the previous data and when close to 0 it will not remember any old data. So, when  $\lambda$  is chosen

according to Equation (7.17e) it depends on  $\frac{\partial s}{\partial t}$  and will therefore not remember any of the previous values when the rail condition is changed. In the same way when the rail condition is persistent the RLS will take previous data into account and therefore be able to estimate a more correct value of the slope  $\hat{k}$ .

To trace the peak point of the slip curve it is enough to use this estimation of the slope. That is since the slope is positive on the stable side and negative on the unstable side of the slip curve. The slope also decreases to zero when the peak is approached. Therefore it is suitable to use the steepest gradient method.

#### Steepest Gradient Method

This method uses the fact that  $\hat{k} = 0$  at the peak of the slip curve. To estimate  $\hat{k} = 0$ , the RLS algorithm with a dynamic forgetting factor is used. When this is done, a slip velocity reference can be calculated according to what is known as the steepest gradient method

$$v_{s_{ref}}(t+1) = v_s(t) + \alpha \hat{k} \quad (7.18)$$

The constant  $\alpha$  is positive.  $v_{s_{ref}}(t+1)$  is the slip velocity reference. This implies an optimal use of the adhesion, as was described in Section 3.3.6.

When we implemented this in MATLAB-SIMULINK we found it to be preferable to separate the two cases when  $\hat{k}$  was positive and negative. The reason is that the slope of the slip curve is different on the stable and unstable side. On the stable side it is almost linear with a large slope in the beginning and a smaller slope when the peak is approaching. On the unstable side on the other hand the slope is large right after the peak and thereafter decreasing. This implies that when we are far away from the peak of the curve on the unstable side,  $\alpha \hat{k}$  is small, but we need it to be large to enable a fast recover to the stable side. With this in mind, we constructed this variant of the steepest gradient method

$$\hat{k} \geq 0 \Rightarrow v_{s_{ref}}(t+1) = v_s(t) + \alpha \hat{k} \quad (7.19a)$$

$$\hat{k} < 0 \Rightarrow v_{s_{ref}}(t+1) = v_s(t) - \beta \quad (7.19b)$$

When we are on the unstable side we use a constant step length to enable a quick recovery. In our simulations we used  $\alpha \approx 2 \times 10^{-8}$  and  $\beta \approx 3 \times 10^{-3}$ .

When the slip velocity reference,  $v_{s_{ref}}(t+1)$ , is calculated it still remains to construct a control signal. This is done by adding the vehicle velocity and dividing with the radius of the wheel according to

$$\frac{v_{s_{ref}}(t+1) + v}{r} = \frac{\omega_{ref}r - v + v}{r} = \omega_{ref} \quad (7.20)$$

When the reference angular velocity  $\omega_{ref}$  is known, a simple P-controller can be used to calculate the reference torque as follows

$$T_{ref} = K_p(\omega_m - \omega_{ref}) \quad (7.21)$$

The complete realization of the RLS with the steepest gradient method is presented in Figure 7.4.

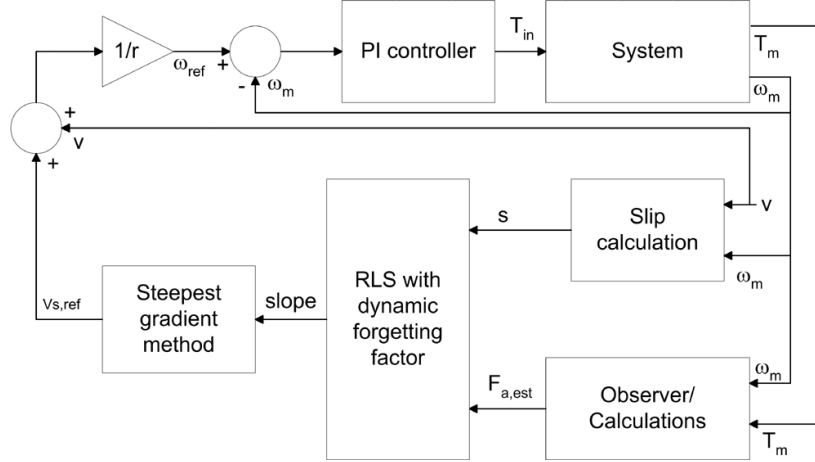


Figure 7.4: Block diagram of the RLS with the steepest gradient method.

## 7.4 Evaluation of Model Based Controllers

The two different methods in Section 7.3.1 and Section 7.3.2 are evaluated in this section. They are tested according to the test cycles presented in Section 5.2.

### 7.4.1 Direct Torque Feedback Control

When we implemented this controller it was not successful. There were mainly two reasons for this. The first came of the fact that the slip curves used in [22] lacked a plateau after the peak. A slip curve with a plateau is shown in Figure 7.5. A plateau, like a peak, implies  $\frac{\partial \mu_a}{\partial t} = 0$  and therefore this controller does not recover once a peak is exceeded and a plateau is entered. This happens because the controller experiences it like it already is at the peak. This is something we found to be a major setback with this control method. The shape of the slip curves is not something that is well known and therefore not a thing that can be taken for granted.



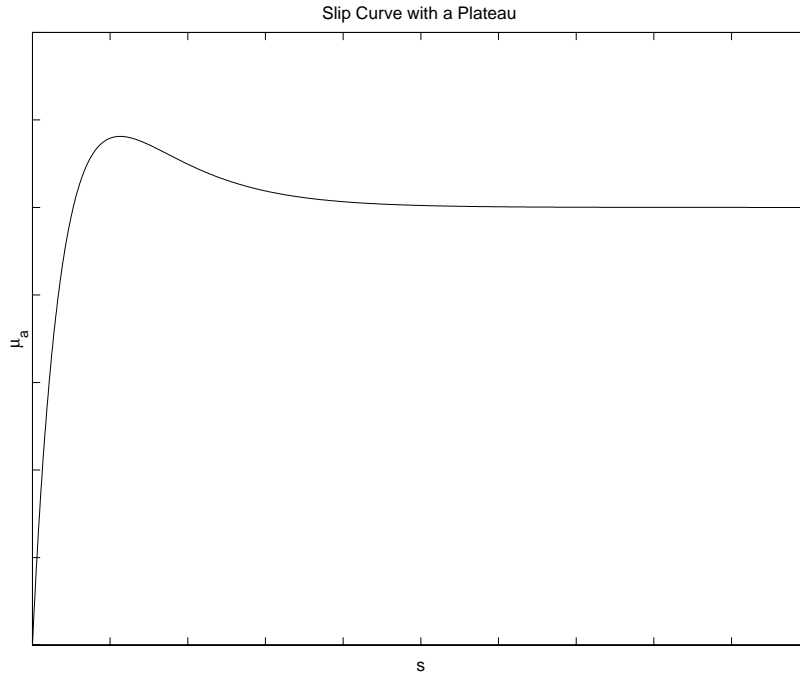


Figure 7.5: Slip curve with a plateau after the adhesion coefficient peak.

The other setback with this method is that it demands an excitation of the system. This shows if the reference torque is set to a fixed value, since when the fixed value is reached,  $\frac{\partial \mu_a}{\partial t}$  will turn to zero. The reason is that there is no longer any changes of the adhesion coefficient in time. This also implies a difficulty and an extra uncertainty.

These two negative factors were the reason why we did not lay the time needed for an implementation that could show reasonable results in the different test cycles. We still believe that this way of detecting the peak of the adhesion curve is interesting. The main reason is that it is often hard to get a reliable value of the vehicle velocity. There are many examples of when a faulty value in the velocity formation have led to a malfunctioning slip control. Being independent of the vehicle velocity is a rare advantage with this method. Maybe it can be used as a complementary part of another slip control method. Thereby, maybe, faults in the vehicle velocity formation can be detected.

#### 7.4.2 RLS with the Steepest Gradient Method

This control method was successfully implemented and tested with the rail condition test and the acceleration test as described in Section 5.2.

### Rail Condition Test

The results of the rail condition test at the speed of 10 km/h is shown in Figure 7.6. We also performed the test with the speed of 40 km/h and this result can be found in Appendix A, Figure A.1.

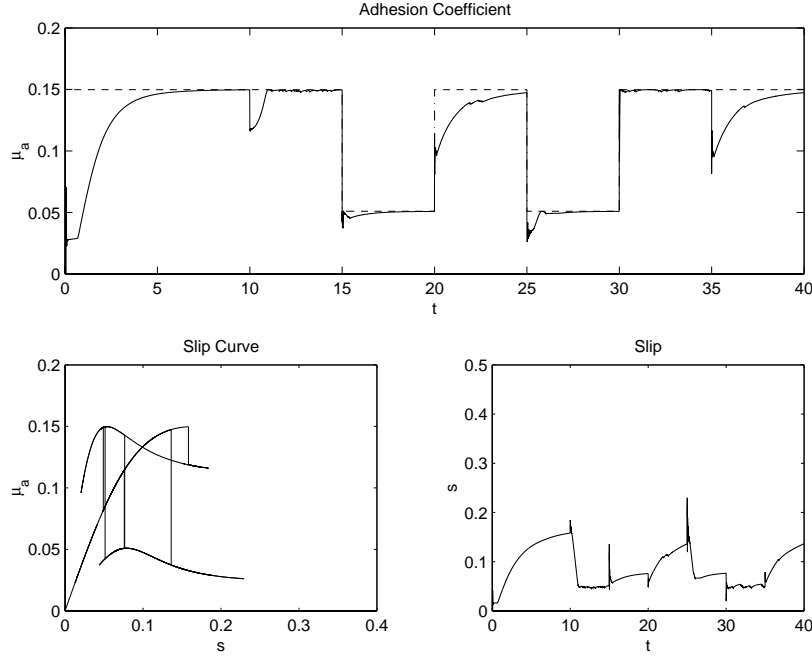


Figure 7.6: The rail condition test for the RLS with the steepest gradient method.

This test starts with curve C for ten seconds. As seen in Figure 7.6, the RLS with the steepest gradient method gets closer and closer to the peak. After ten seconds the rail condition switch to curve A and the controller handles it without any trouble. The next switch take place after 15 seconds from curve A to B. This shift is even more successful than it first looks like, since the recovery from the unstable side to the stable side of the slip curve is instant. In the adhesion coefficient plot in Figure 7.6 it seems like it has not recovered until after about 17 seconds, but it is already on the stable side and working its way up to the optimal value from the stable side. The next switch between curve B and C is no problem either, except that it does not have the time needed to reach the optimal slip. After 25 seconds the most difficult switch from curve C to curve B occurs, but the controller handles it well. After less than one second the controller has recovered to the stable side. If one looks close at the adhesion coefficient plot it is

seen, like before, that it recovers to the stable side and then starts the optimization process. The last switches from curve B to A and from A to C are performed without any problems.

One positive thing with the RLS with the steepest gradient method is that it enables quick recovery into the stable region. Once there, the optimization process starts to maximize the use of the adhesion coefficient. Another great thing with this method is that the RLS in general is robust against noise. A negative thing with the method is that it does not reach the optimal adhesion coefficient for curve C during the five seconds in the rail condition test. The reason is that the different parameters in the RLS, the steepest gradient method and the P-controller is not tuned to their full extent. Still the results are more than satisfying.

#### Acceleration Test

In this test the maximum acceleration was tested on curve B; the one with the lowest adhesion peak of our test curves. The test is presented in Figure 7.7. Here, it is clearly seen that the RLS with the steepest

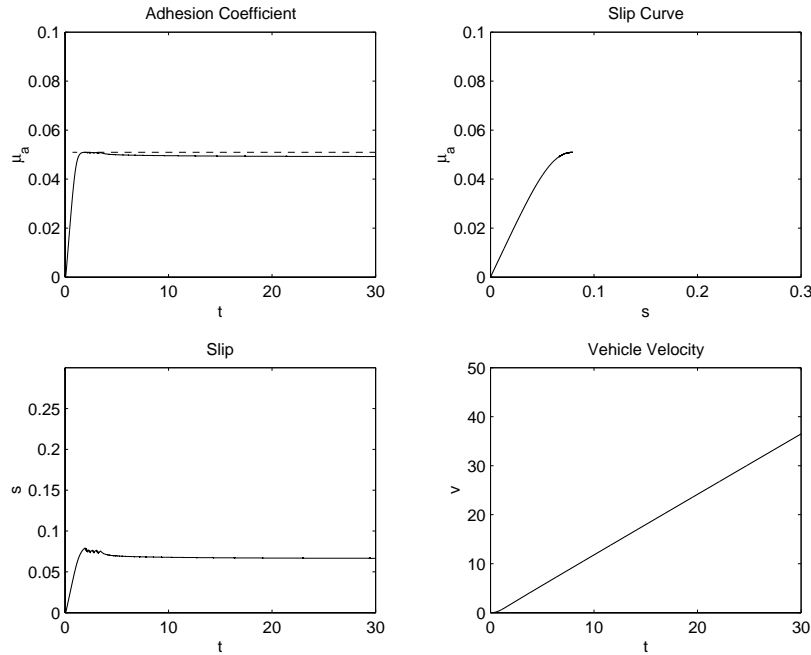


Figure 7.7: The acceleration test for the RLS with the steepest gradient method. In the vehicle velocity plot,  $v$  is measured in km/h.

gradient method performs well. What first may seem like a problem is that in the plot of the adhesion coefficient it almost seems like a stationary fault in the optimization process. This is the natural result of having an optimization controller with non-linear steps of this type. When the vehicle velocity increases, the slip velocity reference is updated with too small steps due to the fact that the peak of the slip curve is near. This result appears like a stationary fault in the adhesion coefficient plot. Once the velocity is constant the controller will have the necessary time to eliminate this small existing fault. Note that this cannot happen on the unstable side, since the recovery is using fixed steps.

## Chapter 8

# Fuzzy Logic Slip Controllers

Fuzzy logic controllers have become very popular in the last few years. Since slipping is a non-linear, time varying process, a non-linear controller may be well suited. This is one of the reasons why fuzzy logic is interesting when it comes to slip control.

We have encountered a few different ways of using a fuzzy controller to control slipping and evaluated two of them. We have also added a third method, combining a few of the ideas we have come in touch with and added a few of our own. The first method uses slip and the slip differential as control signals and the other two uses the differences in adhesive force and slip. Before presenting these theories, we will give a brief description of how to realize a fuzzy logic controller.

### 8.1 Realization of a Fuzzy Logic Controller

A fuzzy logic controller is based on a set of logical rules. The first thing to do when realizing such a controller is to define these rules. An example of such a rule is

*If the slip is positive big and the derivate of the slip is positive big, then the compensation should be positive big.*

This rule has two inputs, the slip and its derivate, and one output, the compensation. To each one of these signals a so called membership function is tied. This function represents a sliding degree of membership. The most common form to be used is a triangular function. Three triangular membership functions called "Negative", "Zero" and

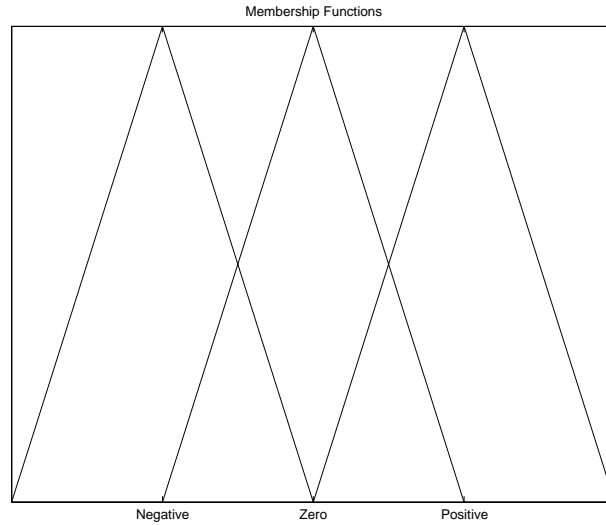


Figure 8.1: Three triangular membership functions, "Negative", "Zero" and "Positive".

"Positive" are shown in Figure 8.1. This figure shows how the degree of membership changes between the three functions. All of this is addressed further in [7] and described in detail in [3].

One way of realizing a fuzzy logic controller is to construct it as a control surface. When doing so, the set of rules are written in a table, similar to the one shown in Table 8.1. This can be translated into a three-dimensional control surface. How the different rules will overlap depend on the shape of the membership functions.

This is a simple and effective way of constructing a non-linear controller. It gives the constructor the freedom of being able to make case-specific adjustments, simply by changing the weight of any membership function in the control structure.

## 8.2 Slip Control Methods using Fuzzy Logic

In the following sections we will describe three different control strategies. The factor they all have in common is the use of fuzzy logic. The first method uses fuzzy logic to produce a fast controller and the latter two for optimization towards the optimal slip, and thereby maximize the adhesive force. Before presenting these methods, we will give a description of the ideas behind such controllers.

The goal of a slip optimizing algorithm is to produce an optimal

slip reference, to be used when controlling the slip. This can be done without knowledge of the actual appearance of the slip curves. By analyzing the time differential of the slip,  $\frac{\partial s}{\partial t}$ , and of the adhesive force,  $\frac{\partial F_a}{\partial t}$ , one can tell if being far from or close to the maximum use of adhesive force. This is illustrated in Figure 8.2.

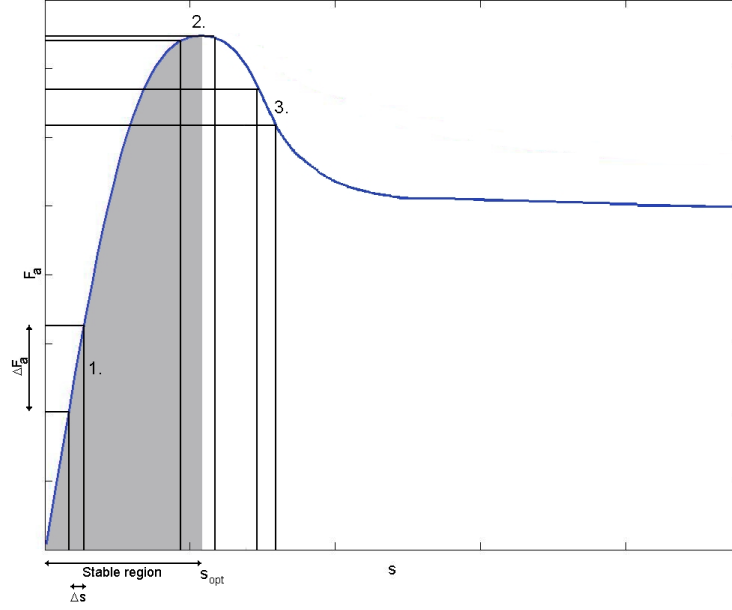


Figure 8.2: The slip optimizing algorithm described in Section 8.2.

1. When  $\frac{\partial F_a}{\partial t}$  is big and positive and  $\frac{\partial s}{\partial t}$  is small and positive, the optimal slip is a higher value than the current value. The same goes for the case when  $\frac{\partial F_a}{\partial t}$  is big and negative and  $\frac{\partial s}{\partial t}$  is small and negative.
2. When  $\frac{\partial F_a}{\partial t}$  is small and  $\frac{\partial s}{\partial t}$  is big, the current slip is close to the optimal slip. If the sign of  $\frac{\partial F_a}{\partial t}$  is equal to the sign of  $\frac{\partial s}{\partial t}$ , then the current position is on the stable region of the adhesion curve.
3. If  $\frac{\partial F_a}{\partial t}$  is big and negative and  $\frac{\partial s}{\partial t}$  is small and positive, or if  $\frac{\partial F_a}{\partial t}$  is big and positive and  $\frac{\partial s}{\partial t}$  is small and negative, the optimal slip is a lower value than the current value.

It is possible to create slip optimizing algorithms using only the sign of  $\frac{\partial F_a}{\partial t}$  and  $\frac{\partial s}{\partial t}$  to decide whether to add or subtract a fixed contribution

to the reference slip. When using fuzzy logic, the size of this contribution can be calculated from a non-linear fuzzy logic control surface. This gives great possibilities to tune the regulator, using different gains in different regions. For instance, if being in the unstable region of the slip curve, maybe the priority to decrease the torque is higher than it is to increase it when being in the stable region. Also, the gain should be higher when being far from the optimum. The fuzzy rule set can be chosen in line with these arguments. This has a lot in common with the steepest gradient method, described in Section 3.3.6.

### 8.2.1 Fuzzy Logic Non-Linear PD-Controller

García-Riviera et al. [6] have successfully implemented a fuzzy logic slip controller on a physical scale model of an electrical locomotive with carriages. We have implemented a similar control structure as a controller for our model described in Chapter 4.

The control structure in use has an outer loop for speed control and an inner loop for slip control (see Figure 8.3). This means the reference to the motor is not the torque wished for, but the speed wished for. The

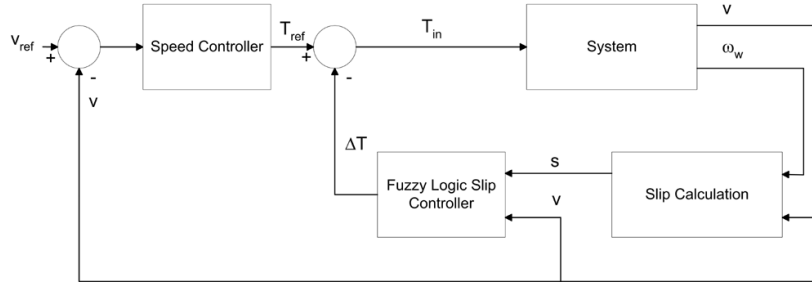


Figure 8.3: The control structure of the fuzzy logic non-linear PD-controller.

speed controller in use is a PI-controller. The input to this controller is the difference between the motor speed wished for and the current speed. When using this type of control structure, the slip will actually be affected by the speed controller, since when the slipping increases, so does the motor speed, and therefore the torque will be reduced. On the other hand, the maximum accessible acceleration will not be used all the way to the speed wished for even when the conditions are good.

The inner loop contains a fuzzy logic control structure. This is based on a table of fuzzy rules, similar to the ones described in Section 8.1. The table of rules in use is shown in Table 8.1. N, P and ZE stands for negative, positive and zero and S, M and B for small, medium and big. These rules are implemented in the control structure as triangular



membership functions. The control surface these rules result in is shown in Figure 8.4.

Table 8.1: The set of rules for the fuzzy logic PD-controller of Section 8.2.1.

$\dot{s} \backslash s$	NB	NM	NS	ZE	PS	PM	PB
NB	NB	NB	NB	NB	ZE	PS	PM
NM	NB	NB	NB	NM	PS	PM	PB
NS	NB	NB	NM	NS	PM	PB	PB
ZE	NB	NM	NS	ZE	PS	PM	PB
PS	NB	NB	NM	PS	PM	PB	PB
PM	NB	NM	NS	PM	PB	PB	PB
PB	NB	NM	NS	PB	PB	PB	PB

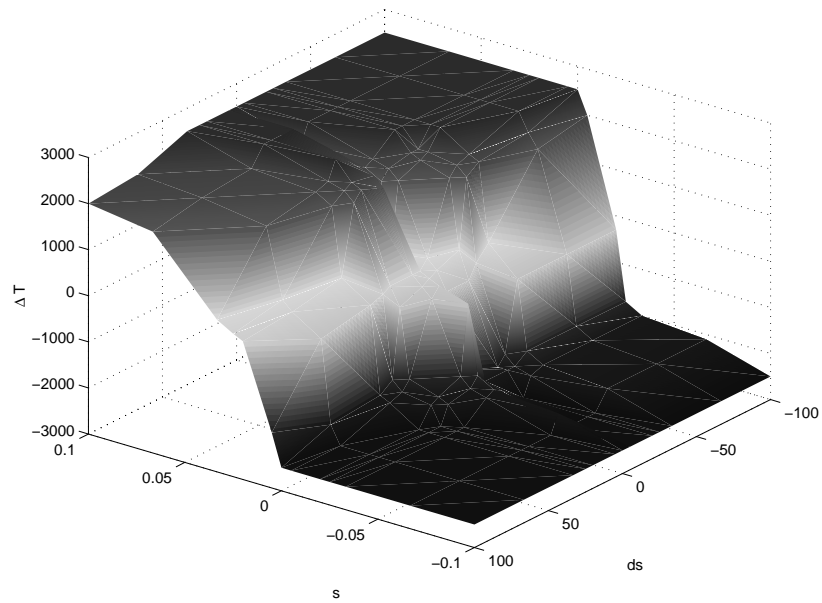


Figure 8.4: The principle appearance of the control surface for the fuzzy logic non-linear PD-controller.

Since the inputs of this controller are slip and the slip differential, the result will become a non-linear PD-controller. This structure will assure fast compensation of torque when far from the optimal slip value and only small compensation when being close. The input slip should be the difference between the optimal slip and the current slip. However, this method provides no information of what really is optimal.

Either a fixed reference slip must be presumed to be optimal or an optimizing algorithm has to be added.

### 8.2.2 Ideal Fuzzy Logic Slip Optimizing Controller

The fuzzy logic controller described in Section 8.2.1 used fuzzy logic to create a non-linear PD-controller. Fuzzy logic can also be used in order to calculate an optimal reference slip, as described in Section 8.2. Palm et al. [23] have used these ideas in order to create a fuzzy logic slip optimizing controller. They use the adhesive force from their process model as a control signal, though this signal is not measurable, which makes this an ideal control structure.

Table 8.2 shows the set of rules used by [23]. They have implemented their control structure on a model of a locomotive. The notation in the table, NB etc, is the same as used in Section 8.2.1. From the set of rules in Table 8.2, a control surface was realized. This is shown in Figure 8.5.

Table 8.2: The set of rules for the slip optimizing controller used by [23].

$\frac{\partial F_a}{\partial t} \setminus \frac{\partial s}{\partial t}$	<b>NB</b>	<b>NS</b>	<b>ZE</b>	<b>PS</b>	<b>PB</b>
<b>NB</b>	PB	PS	ZE	NS	NB
<b>NS</b>	PS	PS	ZE	NS	NS
<b>ZE</b>	ZE	ZE	ZE	ZE	ZE
<b>PS</b>	NS	NS	ZE	PS	PS
<b>PB</b>	NB	NS	ZE	PS	PB

This control surface is a part of the whole control structure, shown in Figure 8.6. In the block called the "Fuzzy Logic Slip Optimizer", the adhesive force and slip are first differentiated and then sent into the fuzzy logic control surface. The output of this surface is a small contribution  $\Delta I$ , positive or negative, which is integrated in order to produce the optimal slip reference. This integration corresponds to the recursive algorithm in the steepest gradient method, Equation (3.5). We found it necessary to low pass filter  $\Delta I$ , in order not to get large signals when there is a sudden change in rail condition. This can probably be avoided by putting more effort into tuning the control surface. When using a low pass filter, this has to be done before integrating the signal. After the integration, the calculated optimal slip is compared with the current slip and sent through a controller. We have tried both P- and PI-controllers. However, the offset is insignificant, and therefore we use the P-controller in our evaluations. The gain in this P-controller has to be very high, since it translates slip error into torque compen-

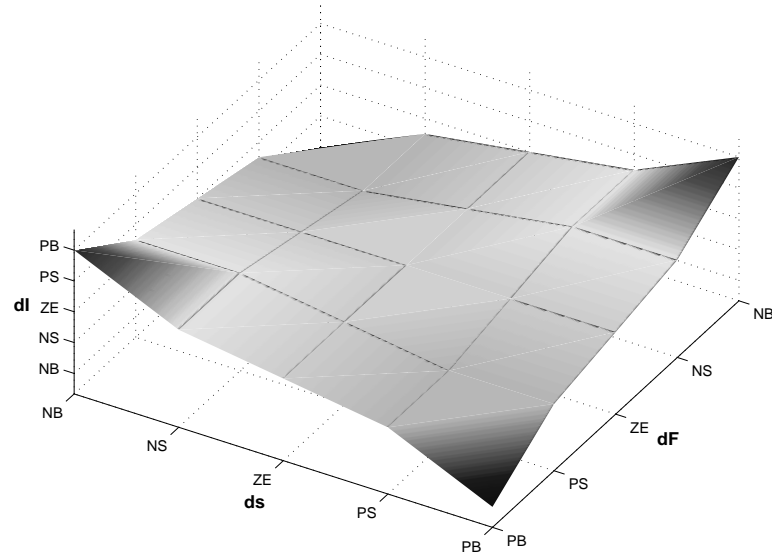


Figure 8.5: The slip optimizing control surface corresponding to the set of rules in Table 8.2.

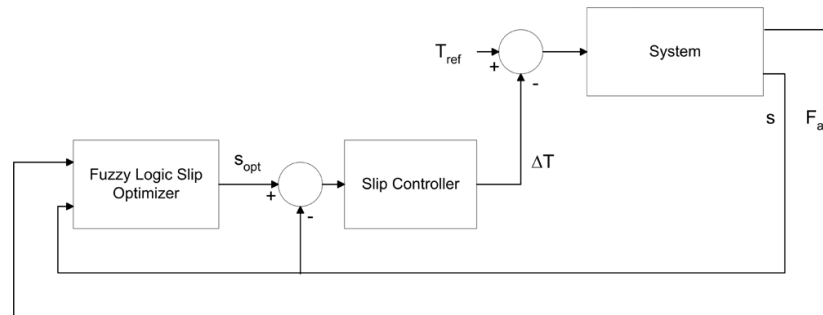


Figure 8.6: The control structure of the ideal slip optimizing fuzzy controller.

sation. The last step is to add this compensation to the torque set by the driver, in order to produce the new reference torque sent to the traction motor.

### 8.2.3 A Novel Fuzzy Slip Optimizing Controller using an Adhesion Observer

The ideal fuzzy logic slip optimizing controller described in Section 8.2.2 works, but it can not be implemented in reality, since the adhesive force is not measurable. Also, the fuzzy logic rule set in use is not optimal for constructing a fast and accurate slip optimizing controller.

We have developed a new, more powerful, fuzzy logic control structure and combined it with the adhesion observer, derived in Section 7.1. Before presenting the details of this work, we will motivate why this has been done.

In Figure 8.2, it is shown how the differences in adhesive force and in slip can be used to determine the current position on the slip curve. This information can be used to create protecting barriers, preventing the adhesive force from dropping down on the unstable side of the slip curve (see Figure 2.3). For instance, if the change in the estimated adhesive force,  $\frac{\partial \hat{F}_a}{\partial t}$ , is negative and big and the change in slip,  $\frac{\partial s}{\partial t}$  is positive and small, we have just dropped over the peak into the unstable region (position 3 in Figure 8.2), and therefore we want the torque to be reduced quickly. Also, when the change in  $\frac{\partial \hat{F}_a}{\partial t}$  is positive and big and the change in slip  $\frac{\partial s}{\partial t}$  is positive and small, we are furthest away from the optimum (position 1 in Figure 8.2). Therefore, the compensating torque should be maximal at this point. This is not the case in the control structure proposed by [23] and presented in Table 8.2 and Figure 8.5.

The discussion above has led to a new control structure (see Figure 8.7) and a new set of rules, presented in Table 8.3. As in the

Table 8.3: The set of rules for the novel slip optimizing fuzzy controller.

$\frac{\partial \hat{F}_a}{\partial t} \setminus \frac{\partial s}{\partial t}$	NB	NM	NS	ZE	PS	PM	PB
NB	PSM	PM	PB	ZE	NB	NM	NSM
NS	PS	PSM	PM	ZE	NS	NSM	NS
ZE	ZE	ZE	ZE	ZE	ZE	ZE	ZE
PS	NS	NSM	NM	ZE	PM	PSM	PS
PB	NSM	NM	NB	ZE	PB	PM	PSM

previous sections, N and P stands for negative and positive, while S, M and B means small, medium and big. SM represents a state between small and medium.

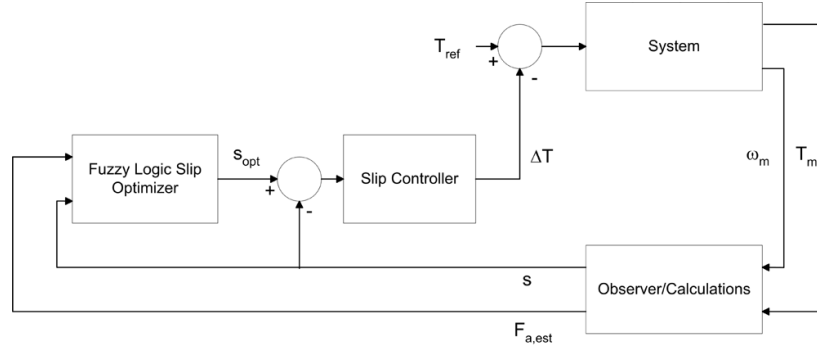


Figure 8.7: The control surface of the novel slip optimizing fuzzy controller.

The new box observer/calculations in Figure 8.7 represents the adhesion observer and the slip calculations. The observer gain  $\frac{\omega_c}{s+\omega_c}$  provides a natural filtering of the estimated adhesive force,  $\hat{F}_a$ . In the box called fuzzy logic slip optimizer, these signals are first derivated and then sent through the fuzzy logic control structure. The output of this structure is a small contribution,  $\Delta I$ , which is integrated to calculate the optimal slip (compare with Section 8.2.2). We saturate  $\Delta I$  before the integration, in order not to get too large signals when there is a sudden change in rail conditions.

Also added in this strategy was a small sinus signal in the reference torque. The thought with this signal was to excite the system if necessary, to avoid the optimizer from getting stuck somewhere that is not optimal on the slip curve. Whether this have any effect or not, we have not looked into any closer.

The content of Table 8.3 represents the principles of the new set of rules, though we used different degrees of the level SM etc. This was however only small deviations from what is shown in the table. The resulting fuzzy logic control surface is shown in Figure 8.8.

### 8.3 Evaluation of the Fuzzy Logic Slip Control Methods

Here, we present the advantages and disadvantages of the control structures described in this chapter. We also present various simulation results. Since the objective in this master's thesis has not been to optimize a specific method, but to compare several different methods, one should keep in mind that none of the controllers have been tuned to the full extent possible.

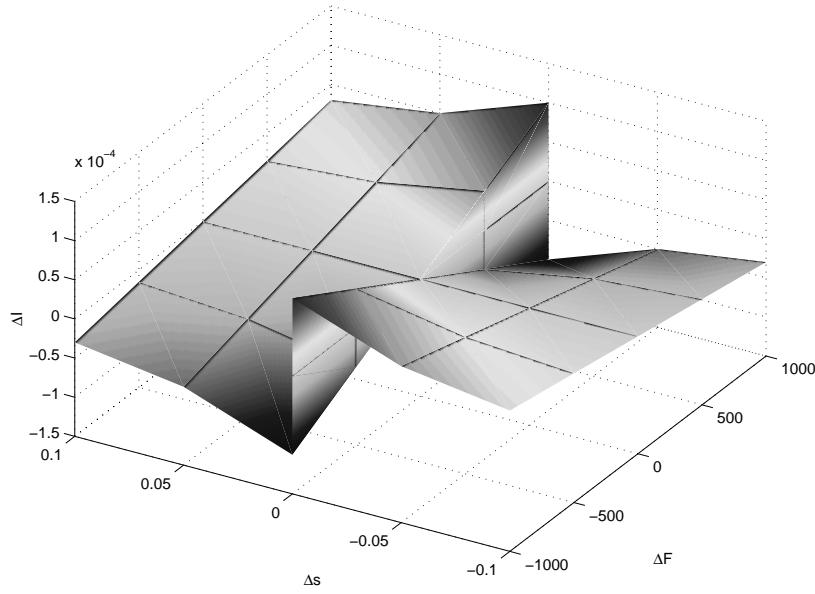


Figure 8.8: The control structure of the novel slip optimizing fuzzy controller.

### 8.3.1 Fuzzy Logic PD-Controller

This section contains the evaluation of the slip control method described in Section 8.2.1. The major advantages and disadvantages of this controller were also mentioned there, but now we will take this discussion one step further. The strength of this non-linear PD-controller is its speed. It is fast when far away from its reference slip and slow when close. The use of a fixed reference slip is the greatest disadvantage. Under the assumption that this reference is close to the real optimal slip, and also that the slip curves behave as assumed, this method will perform very well. We will now present the result of the two tests. The tests performed are described in Section 5.2.

#### Rail Condition Test

The first test performed on the fuzzy logic PD-controller was the rail condition test. Starting after ten seconds, the rail condition is changed every fifth second. Figure 8.9 shows the results of this test when the vehicle velocity was 10 km/h. The results when the velocity was 40 km/h is found in Appendix A, Figure A.2.

As seen in the adhesion coefficient plot, this method is very fast when it comes to convergence towards the reference slip. However, it

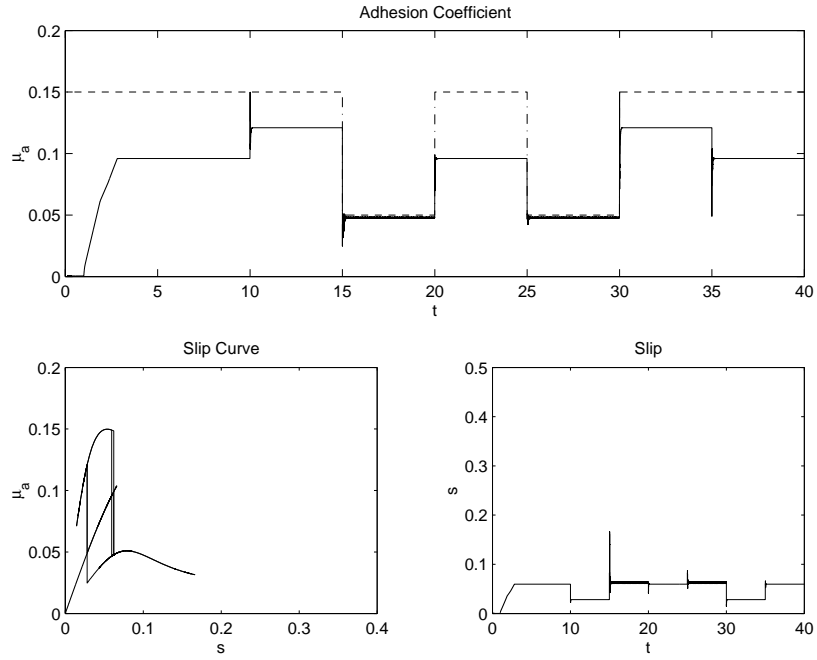


Figure 8.9: The performance of the fuzzy logic PD-controller in the rail condition test, 10 km/h.

can also be seen that it never finds the optimal  $\mu_a$  for any of the different slip curves, though it is close when the optimal slip is 7.9 % (curve B). This is a consequence of the fact that this method works towards a fixed reference slip, i.e. it is not optimizing. This fixed reference seems to agree quite well with the optimal slip of curve B, though the offset is larger for curve A and really large for curve C.

The speed of the controller can also be seen in the slip curve. When changing between the different curves, the slip never exceeds 18 %, and hardly ever even 10 %. The slip plot shows that the 18 % slip occurred when changing from curve B to curve A. Note that this controller never experiences the difficult change from the peak of curve C to the peak of curve B. This comes of the fact that it never stabilizes on the peak of curve C.

#### Acceleration Test

Figure 8.10 shows the result of the acceleration test. Here,  $\mu_a$  comes quite close to its optimal value, though there is a small offset. This is a consequence of the selected slip reference value. Obviously, this value

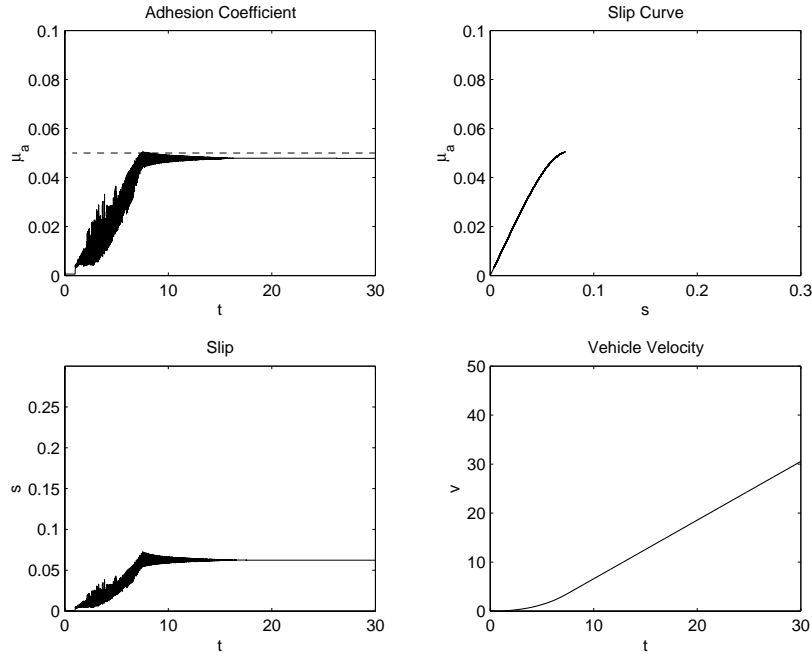


Figure 8.10: The performance of the fuzzy logic PD-controller in the acceleration test. In the vehicle velocity plot,  $v$  is measured in km/h.

works quite well for curve B, which we have already concluded when evaluating the rail condition test. The resulting performance would probably not be very good if the reference slip was for instance three times as big.

Another observation is the a bit nervous behaviour of the slip in the beginning. It takes some time for the controller to determine whether to increase or decrease the compensating torque  $\Delta T$ . Once the velocity has increased to a few km/h, it becomes more stable, and finally fixates  $\Delta T$  at the value in line with what is controlled towards.

With detailed knowledge of the slip curves behaviour, this controller may be unbeatable in speed contra performance, since it can be tuned very precisely. However, as long as such knowledge does not exist, this will just be another fast controller.

### 8.3.2 The Ideal Fuzzy Logic Slip Optimizing Controller

This control strategy represents some of the most interesting ideas we have come in touch with during this master's thesis. It combines the



advantages of an optimizing algorithm with the possibility to use non-linear gain depending on the current position on the slip curve. As mentioned in Section 8.2.2, this method has not been refined to its full extent. During simulation we have seen that it not only works, but also performs very well, though it is by far slower than the novel fuzzy slip optimizing controller of Section 8.2.3. As also mentioned, in the model presented by Palm et al. [23] they have used the adhesive force  $F_a$  as a control signal, which is not possible, since it is not measurable.

We will not present any simulation results of this control strategy, since the optimizing ideas of the control structure are similar to the ones presented in Section 8.2.3, the only difference is that this method performs worse in our tests.

### 8.3.3 The Novel Fuzzy Slip Optimizing Controller using an Adhesion Observer

We will now present the test results of the novel fuzzy slip optimizing controller of Section 8.2.3. There are two major advantages with this method compared to the other methods of this chapter. The first is that it is adhesion optimizing, which the method of Section 8.2.1 is not. The second is that it is based on measurable signals, which the method of Section 8.2.2 is not. The control structure in use provides a much faster optimization than the ones used in Section 8.2.2.

We would like to point out that this controller has only been tuned to the extent that the control signal are of reasonable size. Therefore there are room for a lot of improvements when it comes to tuning.

#### Rail Condition Test

The results of the rail condition test with vehicle velocity 10 km/h is shown in Figure 8.11. The same test performed in 40 km/h is presented in Appendix A.3. Figure 8.11 shows that the optimizing algorithm not only works, but also works fast. The first optimum was reached after only 1.8 seconds. The longest interval ever to occur was when changing from curve C to curve B, which took 2.5 seconds. When this happened we reached the slip 30 %, which was the largest slip ever to occurred in this test. This can probably be reduced quite a bit if a higher gain is used in the fuzzy logic control surface when the change in slip,  $\frac{\partial s}{\partial t}$ , is positive and big and the change in the estimated adhesive force,  $\frac{\partial \hat{F}_a}{\partial t}$ , is negative and small. Note that this was the only time the slip ever exceeded 18 %!

The calculation of the optimal reference slip is the most time consuming part of this controller. The gain of the P-controller controlling the slip towards the optimal reference slip is high, and will not provide any noticeable time delay to the process. If the reference slip where

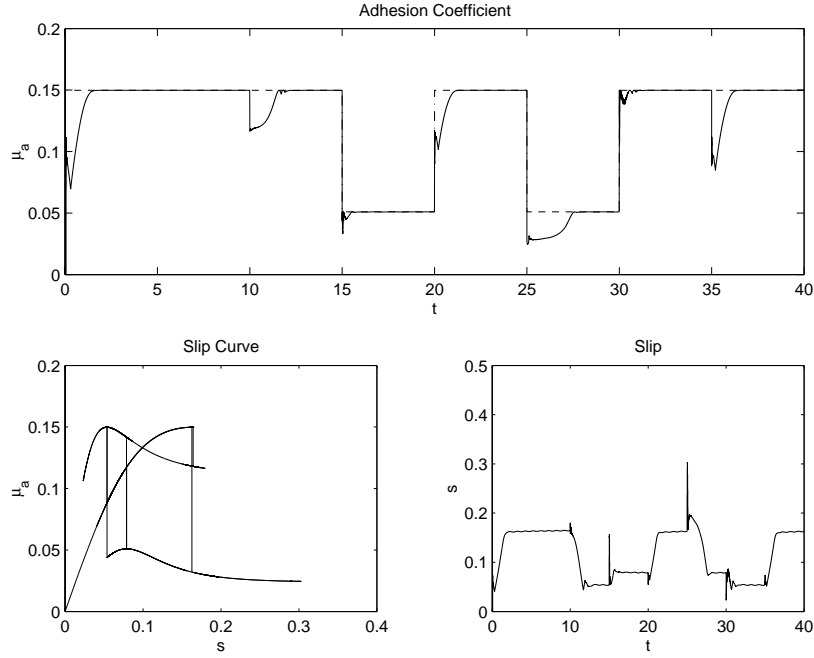


Figure 8.11: The performance of the novel fuzzy slip optimizing controller in the rail condition test, 10 km/h.

to be added in the slip plot, this signal and the slip signal would be almost identical. This comes of the fact that the offset is insignificant, as mentioned in Section 8.2.2.

The result of the rail condition test conducted with the vehicle velocity constant at 40 km/h (Appendix A, Figure A.3) is quite similar to the test done at 10 km/h, only optimizing a lot faster. Here, the maximum slip ever to occur was merely 20 %. This happened when changing from curve C to curve B, just like when the test was performed with the velocity 10 km/h. The the longest optimizing time was around 2.0 seconds, which happened when changing from curve C to curve A.

The fact that the maximum slip is lower and the optimization times are shorter when the vehicle velocity is higher is a result of the slip definition, Equation (2.1). Since the vehicle velocity is the normalizing factor in this definition, it will take a larger change in wheel velocity to cause a certain slip at a higher than a lower vehicle velocity.

### Acceleration Test

Figure 8.12 shows the results of the acceleration test performed on our optimizing fuzzy logic slip controller. The slip curve shows that the con-

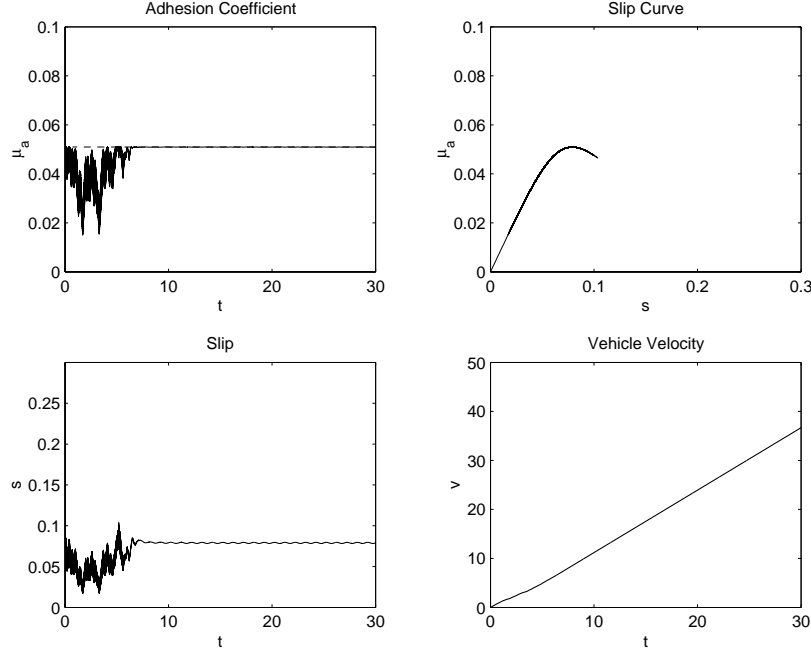


Figure 8.12: The performance of the novel fuzzy slip optimizing controller in the acceleration test. In the vehicle velocity plot,  $v$  is measured in km/h.

troller reacted very quickly when exceeding the optimal value. It is a bit oscillative the first few seconds, just like the non-linear PD-controller evaluated in Section 8.3.1. However, the final velocity reached by this optimizing controller is approximately 24 % higher than the final velocity of the non-linear PD-controller. The small oscillations that can be seen in the slip plot comes from the generated sinus signal we use to excite the system, see Section 8.2.3.

As shown in the tests, our optimizing fuzzy logic slip controller is very fast and very accurate, even though it has not been tuned to the extent possible by far. In Chapter 9, we will briefly compare the methods of this chapter with the methods from Chapter 6 and Chapter 7.



## Chapter 9

# Conclusions and Future Improvements

In this chapter we will summarize the advantages and disadvantages of the methods described in Chapter 6–8. We will propose a few improvements and present ideas that may be interesting in future research.

The major problem when it comes to slip control today is the low reliability in the calculated vehicle velocity. As described in Section 3.1, this comes of the fact that most railway vehicles have mechanical brakes on all the shafts, since it is considered low-cost. The intention is of course to increase security, but this is not achieved if the calculated vehicle velocity cannot be trusted when breaking hard. We have briefly looked at alternative solutions to this problem, but did not find any well working realistic alternatives. As presented in Section 5.1.4, not even the scientists working with speed sensorless control believe it yet to be possible to achieve the same results with as without speed sensors. Our recommendation to overcome this problem is to always have at least one non-driven and non-breaking shaft in all railway vehicles.

Looking back at the slip control methods in this master's thesis, two of them are more interesting than the others. These two methods are the RLS with the steepest gradient method of Section 7.3.2 and the novel fuzzy slip optimizing controller of Section 8.2.3. They can be classified as non-linear slip optimizing control methods; they both use non-linear gain, where the gain is set by their current position on the slip curve. We believe both of these methods to have great future potential as slip controllers.

The hybrid slip control method of Chapter 6 provides a good foundation for a control structure. The pattern control makes a good redundancy if an optimizing slip controller for some reason should malfunction and the acceleration criterion will prevent all-shaft slipping. In its

present shape, this method is not optimizing. It may perform well if bad rail conditions seldom occur, but hardly under rougher conditions. This goes for all of the non-optimizing methods we have evaluated. As long as measurements have not confirmed every possible rail condition, we believe optimizing algorithms should be used for effective performance.

Many attempts have been made to achieve optimizing slip controllers with algorithms similar to the steepest gradient method. Most of these attempts use some exceptional case when the algorithm comes near the peak of the slip curve. This is done to avoid dividing by zero when calculating  $\frac{\partial \mu_a}{\partial s} = \frac{\partial \mu_a}{\partial t} / \frac{\partial v_s}{\partial t}$ . An example of such an attempt is the direct torque feedback method of Section 7.3.1. The RLS and the novel fuzzy method provides much classier solutions to this problem.

When it comes to the RLS with the steepest gradient method, this is not an unique solution. Instead of using RLS with a dynamic forgetting factor, a Kalman filter with a CUSUM-detector can be used. In the same way that the forgetting factor is reduced when a change in the rail condition occur, the CUSUM-detector will change the priority of the Kalman filter. This was not evaluated in this report but it is something that can be addressed in future works.

The non-linear PD-controller of Section 8.2.1 is a fast controller, but then again not optimizing. It can of course be combined with some optimizing slip calculation, but we doubt this would improve much, since the optimization is the slow process in such a control structure and not controlling towards the optimal reference. This fact places this controller in the same category as the hybrid slip control method; it will perform very well if knowing which reference to use.

The novel fuzzy logic slip optimizing controller also have a lot of room for improvements. If putting more effort in developing a smother and more detailed control surface, it is possible to tune the behaviour of this controller to optimize the gain when being at any position of a slip curve.

The RLS with the steepest gradient method and the novel fuzzy logic slip optimizing controller are with no doubt the best performing controllers evaluated in this master thesis. Although they perform so well without being properly tuned, there are still room for improvements.

# References

- [1] E. Andersson and M. Berg. *Järnvägssystem och spårfordon*. KTH Högskoletryckeri, Stockholm, Sweden, August 1999. In Swedish.
- [2] A.D. Cheok and S. Shiomi. Combined heuristic knowledge and limited measurement based fuzzy logic antiskid control for railway applications. *IEEE Transactions on systems, man and cybernetics*, 30(4):557–568, November 2000.
- [3] D. Driankov, H. Hellendoorn, and M. Reinfrank. *An Introduction to Fuzzy Control*. Springer, Munich, Germany, 2nd, revised edition, 1996.
- [4] E. Frisk and M. Nyberg. *Diagnosis and Supervision of Technical Processes*. 2002.
- [5] T. Gadjár, I. Rudas, and Y. Suda. Neural network based estimation of friction coefficient of wheel and rail. *1997 IEEE International Conference on Intelligent Engineering Systems*, pages 315–318, September 1997.
- [6] M. García-Riviera, R. Sanz, and J.A. Pérez-Rodríguez. An antislipping fuzzy logic controller for a railway traction system. *Proceedings of the Sixth IEEE International Conference on Fuzzy Systems*, 1:119–124, 1997.
- [7] T. Glad, S. Gunnarson, L. Ljung, T. McKelvey, A. Stenman, and J. Löfberg. *Digital Styrning, Kurskompendium*. Bokakademien, Linköping, Sweden, 2002. In Swedish.
- [8] T. Glad and L. Ljung. *Reglerteknik. Grundläggande teori*. Studentlitteratur, Lund, Sweden, 2 edition, 1989. In Swedish.
- [9] F. Gustafson. Monitoring tire-road friction using the wheel slip. *IEEE Control Systems Magazine*, 18(4):42–49, August 1998.
- [10] F. Gustafsson. Slip-based estimation of tire - road friction. Technical Report LiTH-ISY-R-1755, Department of Electrical Engineering, Linköping University, Linköping, Sweden, 1995.

- [11] F. Gustafsson, L. Ljung, and M. Millnert. *Signalbehandling*. Studentlitteratur, Lund, Sweden, 2 edition, 2001. In Swedish.
- [12] J-O. Hahn, R. Rajamani, and L. Alexander. Gps-based real-time identification of tire-road friction coefficient. *IEEE Transactions on Control Systems Technology*, 10(3):331–343, May 2002.
- [13] Y. Ishikawa and A. Kawamura. Maximum adhesive force control in super high speed train. *IEEE, Proceedings of the Power Conversion Conference, Nagaoka 1997*, 2:951–954, August 1997.
- [14] S. Kadowaki, K. Ohishi, I. Miyashita, and S. Yasukawa. Re-adhesion control of electric motor coach based on disturbance observer and sensor-less vector control. *IEEE, Proceedings of the Power Conversion Conference, 2002*, 3:1020–1025, April 2002.
- [15] A. Kawamura, K. Takeuchi, T. Furuya, Y. Takaoka, K. Yoshimoto, and M. Cao. Measurement of the tractive force and the new adhesion control by the newly developed tractive force measurement equipment. *IEEE, Proceedings of the Power Conversion Conference*, 2:879–884, April 2002.
- [16] W-S. Kim, Y-S. Kim, J-K. Kang, and S-K. Sul. Electro-mechanical re-adhesion control simulator for inverter-driven railway electric vehicle. *Conference Record of the 1999 IEEE Industry Applications Conference*, 2:1026–1032, 1999.
- [17] P. Liljas. Speed and positioning systems. The traditional way. *IEEE Colloquium on Where Are We Going? (And How Fast!) Seminar Exploring Speed And Positioning Systems For The Transport Sector*, pages 2/1–2/9, November 1997.
- [18] L. Ljung. *System Identification - Theory For the User*. Prentice-Hall, Upper Saddle River, NJ, USA, 2 edition, 1999.
- [19] L. Nielsen and L. Eriksson. *Course material Vehicular Systems*. Linköping, Sweden, 2001.
- [20] K. Ohishi, I. Miyashita, K. Nakano, and S. Yasukawa. Anti-slip control of electric motor coach based on disturbance observer. *IEEE, 5th International Workshop on Advanced Motion Control*, pages 580–585, June 1998.
- [21] K. Ohishi, Y. Ogawa, I. Miyashita, and S. Yasukawa. Adhesion control of electric motor coach based on force control using disturbance observer. *IEEE, Advanced Motion Control*, pages 323–328, April 2000.



- [22] K. Ohishi, Y. Ogawa, I. Miyashita, and S. Yasukawa. Anti-slip re-adhesion control of electric motor coach based on force control using disturbance observer. *IEEE, Industry Applications Conference, 2000*, 2:1001–1007, April 2000.
- [23] R. Palm and K. Storjohann. Torque optimization for a locomotive using fuzzy logic. *Proceedings of the 1994 ACM symposium on Applied Computing*, pages 105–109, April 1994.
- [24] D-Y. Park, M-S. Kim, D-H. Hwang, and Y-J. Kim J-H. Lee. Hybrid re-adhesion control method for traction system of high-speed railway. *IEEE, Proceedings of the Fifth International Conference on Electrical Machines and Systems*, 2:739–742, August 2001.
- [25] O. Polách. Rad-schiene-modelle in der simulation der fahrzeug- und antriebesdynamik. *eb - Elektrische Bahnen*, (5):219–230, 2001. In German.
- [26] H. Sado, S. Sakai, and Y. Hori. Road condition estimation for traction control in electric vehicle. *Proceedings of the IEEE International Symposium on Industrial Electronics, 1999*, 3:973–978, July 1999.
- [27] S. Senini, F. Flinders, and W. Oghanna. Dynamic simulation of wheel-rail interaction for locomotive traction studies. *Proceedings of the 1993 IEEE/ASME Joint Railroad Conference*, pages 27–34, April 1993.
- [28] Y. Takaoka and A. Kawamura. Disturbance observer based adhesion control for shinkansen. *IEEE, Proceedings, 6th International Workshop on Advanced Motion Control, 2000*, pages 169–174, March 2000.
- [29] T. Watanabe and M. Ogasa. Realization of anti-slip/slide control in railway motor vehicles by slip velocity feedback torque control. *IEEE, Fifth European Conference on Power Electronics Applications*, 6:156–161, September 1993.
- [30] T. Watanabe, A. Yamanaka, T. Hirose, and S. Nakamura. Optimization of readhesion control of Shinkansen trains with wheel-rail adhesion prediction. *IEEE, Proceedings of the Power Conversion Conference, Nagaoka 1997*, 1:47–50, August 1997.
- [31] T. Watanabe and M. Yamashita. Basic study of anti-slip control without speed sensor for multiple motor drive of electric railway vehicles. *IEEE, Proceedings of the Power Conversion Conference*, 3:1026–1032, April 2002.

- [32] I. Yasuoka, T. Henmi, Y. Nakazawa, and I. Aoyama. Improvement of re-adhesion for commuter trains with vector control traction inverter. *IEEE, Proceedings of the Power Conversion Conference, Nagaoka 1997*, 1:51–56, August 1997.

# Notation

## Variables and parameters

$a$	Acceleration
$a_i$	Acceleration of bogie $i$
$A$	Maximum vehicle cross section area
$b_t$	Coefficient of the viscous friction in the gearbox
$C_0$	Aerodynamic coefficient for phenomenon independent of $v^2$
$C_d$	Air resistance coefficient
$C_l$	Aerodynamic coefficient depending on objects along a railway vehicle
$C_p$	Aerodynamic coefficient depending on the shape of the front section
$C_{r1}$	Coefficient depending on wheel characteristics
$C_{r2}$	Coefficient depending on wheel characteristics
<i>Curve A</i>	A slip curve with $\mu_{a,max} = 15.0\%$ at $s = 5.4\%$
<i>Curve B</i>	A slip curve with $\mu_{a,max} = 5.1\%$ at $s = 7.9\%$
<i>Curve C</i>	A slip curve with $\mu_{a,max} = 15.0\%$ at $s = 16.5\%$
$F_a$	Adhesive force
$F_{a,w}$	Adhesive force of a specific wheel
$F_{air}$	Air drag
$F_c$	Cornering loss
$F_{loss}$	Force loss
$F_r$	Roll resistance
$g$	Gravity acceleration
$i_t$	Conversion ratio of the gearbox
$J_{lw}$	Moment of inertia of the left wheel
$J_m$	Moment of inertia of the motor
$J_{rw}$	Moment of inertia of the right wheel
$J_t$	Moment of inertia of the gearbox
$J_{tot}$	Total moment of inertia of a mechanical transmission
$K_I$	Integrating gain of a PI-controller
$K_m$	Spring constant of the motor shaft
$K_p$	Proportional gain of a PI-controller
$K_t$	Spring constant of the drive shaft
$L_t$	Length of the railway vehicle

---

$m_a$	Adhesive mass
$m_{a,w}$	Adhesive mass on a specific wheel
$m_{tot}$	Total vehicle mass
$m_w$	Wheel mass
$N$	Normal force
$q$	Total ventilation flow
$r$	Radius of a wheel
$s$	Slip
$s_i$	Slip of bogie $i$
$s_{ref}$	Reference slip
$t$	Time
$T_a$	Adhesive torque
$T_l$	Torque loss
$T_{lw}$	Wheel torque, left wheel
$T_m$	Motor torque
$T_{PI}$	Compensating torque of a PI-controller
$T_{ref}$	Reference torque
$T_{rw}$	Wheel torque, right wheel
$T_t$	In going torque to the gearbox
$T_w$	Wheel torque
$v$	Vehicle velocity
$v_i$	Velocity of shaft $i$
$v_a$	Average velocity
$v_{a,i}$	Average velocity of bogie $i$
$v_{ref}$	Reference velocity
$v_s$	Slip velocity
$v_{s,ref}$	Reference slip velocity
$\alpha$	Coefficient used in the steepest gradient method
$\beta$	Fixed contribution used in the steepest gradient method
$\Delta T$	Compensating torque
$\Delta T_i$	Compensating torque for bogie $i$
$\zeta_m$	Damping of the motor shaft
$\zeta_t$	Damping of the drive shaft
$\theta_{lw}$	Angle of the left wheel
$\theta_m$	Motor angle
$\theta_{rw}$	Angle of the right wheel
$\theta_{t,in}$	Ingoing gearbox angle
$\theta_{t,out}$	Outgoing gearbox angle
$\theta_w$	Wheel angle
$\mu$	Friction coefficient
$\mu_a$	Adhesion coefficient
$\mu_{a,max}$	The maximum value of the adhesion coefficient
$\rho_{air}$	Air density
$\tau$	Time constant of the traction motor
$\varphi$	Slope of the track

---

$\omega$	Angular velocity of a wheel
$\omega_c$	Cut-off frequency
$\omega_{min}$	Lowest angular wheel velocity
$\omega_{max}$	Highest angular wheel velocity

### Operators

$min$	Minimum of argument
$max$	Maximum of argument
$s$	Laplace operator
$\partial$	Partial derivate
$\Rightarrow$	Implies
$\Leftrightarrow$	If and only if



## Appendix A

# Rail Condition Test, 40 km/h

In this appendix the results of the rail condition test (see Section 8.3.1) performed in 40 km/h are presented.

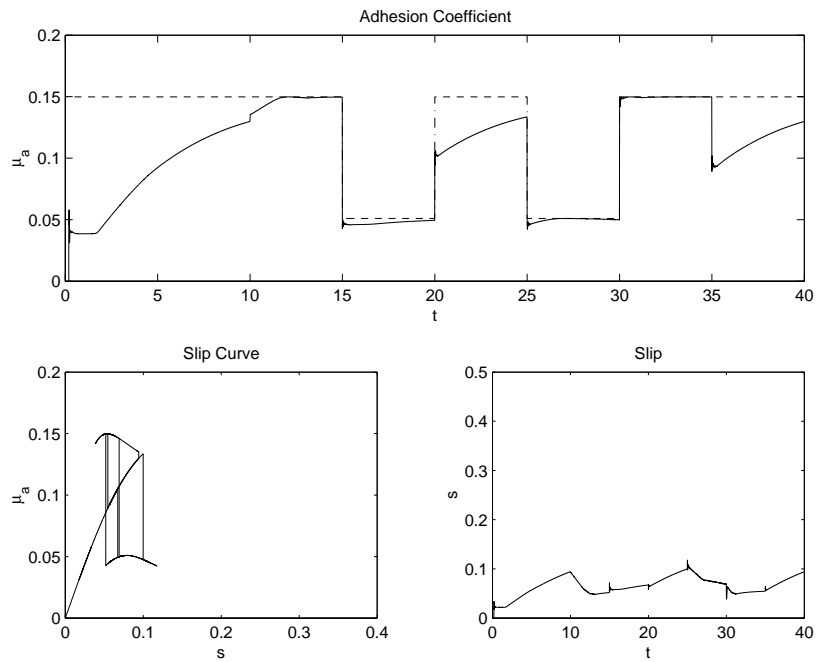


Figure A.1: The Rail Condition Test for the RLS with the Steepest Gradient Method.

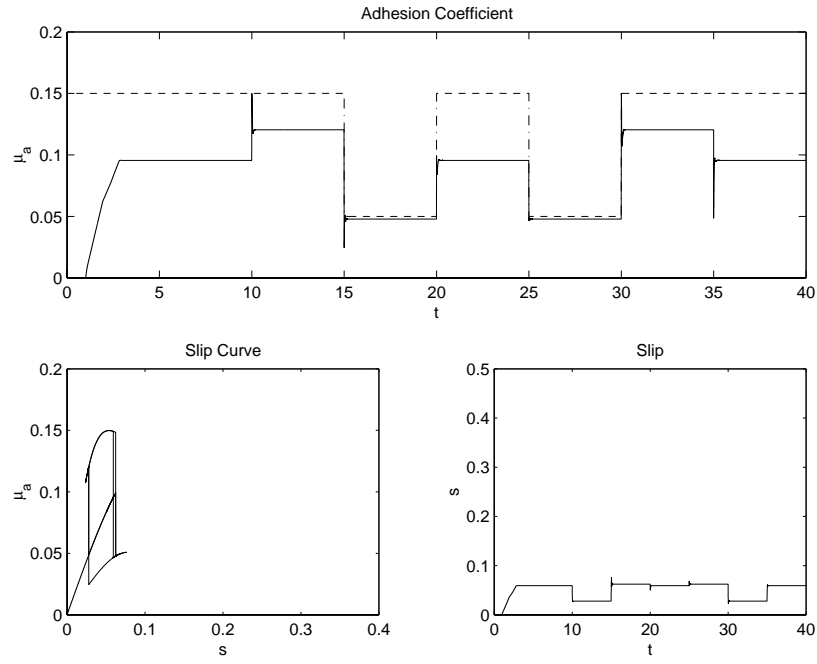


Figure A.2: The rail condition test performed at the fuzzy PD-controller in 40 km/h. For details, see Section 8.3.1



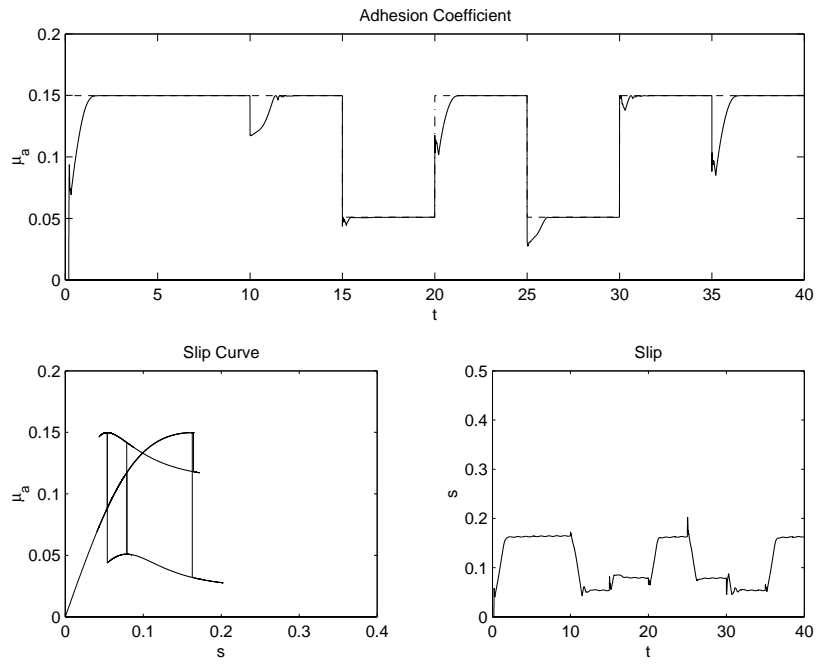


Figure A.3: The rail condition test performed at the novel fuzzy slip optimizing controller in 40 km/h. For details, see Section 8.3.3



# Index

- Acceleration criterion, 40
- Acceleration test, 36, 51, 63, 67
- Adaptive identification algorithm, 44
- Adhesion, 10
- Adhesion coefficient, 27
- Adhesion coefficient, 11
- Adhesion maximum, 12
- Adhesion observer, 20, 41, 60
- Adhesion peak, 42
- Adhesive force, 10, 26
- Adhesive mass, 11
- Adhesive torque, 26
- Air resistance, 28
- Average velocity, 38
- Bogie, 38
- Calibration, 16
- Cars, 29
- Conclusions, 69
- Control strategies, 18
- Control surface, 54
- Cornering loss, 28
- Cut-off frequency, 42
- Damping coefficient, 24
- Deformation, 9
- Determine the velocity, 15
- Diagnostic algorithms, 18
- Direct torque feedback method, 43
- Drive shaft, 16
- Dynamic forgetting factor, 46
- Electrical multiple unit, 29
- Fixed steps, 39
- Friction force, 10
- Future improvements, 69
- Fuzzy logic, 21
- Fuzzy logic slip controllers, 34, 53
- Fuzzy rule set, 53
- Gearbox, 24
- Goal of slip control, 12
- GPS, 17
- Hybrid slip control method, 20, 33, 37
- Ideal fuzzy controller, 58
- Linguistic rules, 21
- Loss due to roll, 28
- Measurable, 58
- Mechanical brakes, 15
- Mechanical transmission, 23
- Membership functions, 53
- Method criticism, 4
- Methods not further evaluated, 34
- Minimum velocity, 37
- Model based controllers, 19, 34, 41
- Moment of inertia, 24
- Motor current differences, 19
- Neural networks, 18
- Non-driven shaft, 37
- Non-linear PD-controller, 56
- Normal force, 9

- 
- Novel fuzzy controller, 60
  - Objectives, 3
  - Optimal slip, 13
  - Optimal use of adhesion, 60
  - Optimizing algorithm, 54
  - Organisation, 4
  - OTU, 29
  - Outer conditions, 26
  - Outer losses, 28
  - Pattern control, 39
  - Pattern control method, 19
  - Peak of the slip curve, 13
  - PID limitations, 21
  - Plateau, 48
  - Pressure sensor, 16
  - Pulse calculation, 16
  - Rail condition test, 35, 50, 62, 65
  - Realizing fuzzy logic, 53
  - Reduced mechanical transmission, 42
  - Reference torque, 24
  - Report disposition, 6
  - RLS, 44
  - Sinus signal, 61
  - Slide, 9
  - Slip, 9, 27
  - Slip velocity, 9, 27
  - Slip curve, 12, 26, 35
  - Slip detection, 17
  - Slope, 43, 44
  - Speed difference method, 17, 38
  - Speed sensorless, 19
  - Speed sensors, 16
  - Spring constant, 24
  - Stable region, 12, 44
  - Steepest gradient method, 20
  - Target group, 5
  - Test curves, 35
  - Test cycles, 35
  - Thesis background, 3
  - Thesis methods, 3
  - Threshold, 18, 39
  - Time plan, 5
  - Torque command function, 44
  - Total mass, 28
  - Traction motor, 23
  - Unstable region, 12, 60
  - Variable steps, 39
  - Vehicle velocity, 12, 28
  - Viscous friction, 24
  - Wheel profile, 16
  - Wheel radius, 26
  - Wheels, 25